Space Sci Rev (2016) 205:231–265
DOI 10.1007/s11214-016-0248-1

Insights into Planet Formation from Debris Disks

II. Giant Impacts in Extrasolar Planetary Systems

Mark C. Wyatt[1] · **Alan P. Jackson**[2]

Received: 18 September 2015 / Accepted: 14 March 2016 / Published online: 22 March 2016

Abstract *Giant impacts* refer to collisions between two objects each of which is massive enough to be considered at least a planetary embryo. The putative collision suffered by the proto-Earth that created the Moon is a prime example, though most Solar System bodies bear signatures of such collisions. Current planet formation models predict that an epoch of giant impacts may be inevitable, and observations of debris around other stars are providing mounting evidence that giant impacts feature in the evolution of many planetary systems. This chapter reviews giant impacts, focussing on what we can learn about planet formation by studying debris around other stars. Giant impact debris evolves through mutual collisions and dynamical interactions with planets. General aspects of this evolution are outlined, noting the importance of the collision-point geometry. The detectability of the debris is discussed using the example of the Moon-forming impact. Such debris could be detectable around another star up to 10 Myr post-impact, but model uncertainties could reduce detectability to a few 100 yr window. Nevertheless the 3 % of young stars with debris at levels expected during terrestrial planet formation provide valuable constraints on formation models; implications for super-Earth formation are also discussed. Variability recently observed in some bright disks promises to illuminate the evolution during the earliest phases when vapour condensates may be optically thick and acutely affected by the collision-point geometry. The outer reaches of planetary systems may also exhibit signatures of giant impacts, such as the clumpy debris structures seen around some stars.

Keywords Circumstellar disks · Planet formation

1 Introduction

The majority of the processes that contribute to the formation of a planetary system are thought to take place in the massive circumstellar disks that surround young stars called

✉ M.C. Wyatt
wyatt@ast.cam.ac.uk

[1] Institute of Astronomy, University of Cambridge, Madingley Road, Cambridge CB3 0HA, UK

[2] School of Earth and Space Exploration, Arizona State University, Tempe, AZ 85287, USA

protoplanetary disks. Such disks last for up to around 10 Myr before dispersing through mechanisms that are still debated, leaving a planetary system and a debris disk (Wyatt et al. 2015). The debris disk is made up of the components of the planetary system that are not massive enough to be classed as planets, i.e., planetesimals, dust and gas (see Matthews et al. 2014). For example, the Asteroid Belt and Kuiper Belt account for the majority of Solar System's debris disk, along with the Zodiacal Cloud and the Oort Cloud (see e.g., Matthews and Kavelaars 2016).

The motivation for saying that planet formation processes are largely complete by the time the protoplanetary disk is dispersed is based on the absence of large quantities of gas and dust at later stages from which to form planets (e.g., Haisch et al. 2001). However, while the disappearance of the protoplanetary gas disk does make the formation of gas giant planets like Jupiter rather problematic, this does not necessarily prevent the continued growth of solid rocky or icy planets. From an observational perspective we can only say that the mass present in less than cm-sized dust cannot be significant after the protoplanetary disk has dispersed (Panić et al. 2013). The majority of the solid mass in the system could instead be locked up in planets (or planetary embryos) that continue to grow. Indeed this is the basis of some models for planetary system formation and evolution that aim to explain some debris disk observations (Kenyon and Bromley 2008).

Isotopic compositions indicate that the parent bodies of many of the meteorites formed within the first few Myr of the Solar System's history (e.g. Kleine et al. 2009), i.e., while the protoplanetary disk would have still been present. However, a lengthier timescale for the formation of solid rocky planets is inferred from isotopic measurements of the terrestrial planets, which shows that they formed over a range of timescales, with Earth taking up to ~ 100 Myr to reach its final mass (e.g. Halliday 2008). The long formation timescale for the Earth is readily understood within the context of favoured models for planet formation. In such models, the protoplanetary disk is suffused with planetesimals that grow via mutual collisions to eventually become planets, with a system of terrestrial planets that bears many similarities to our own inner Solar System a likely outcome for the right initial conditions (e.g., Hansen 2009; Walsh et al. 2011). Of relevance to the current discussion is that planetesimal growth results in many planetary embryos (Kokubo and Ida 1998), and in the final stage the number of embryos is whittled down to a few as they undergo repeated chaotic close encounters and eventually giant collisions, until the few that remain are sufficiently separated to be dynamically stable (e.g., Goldreich et al. 2004; Kenyon and Bromley 2006). One consequence of this scenario is that the formation of the Earth's moon in a giant impact ~ 100 Myr after the Solar System formed is not an atypical occurrence.

The detailed structures of other inner Solar System bodies also bear witness to a past epoch of giant (i.e., planetary scale) impacts in the inner Solar System (e.g., Benz et al. 1988; Marinova et al. 2011). There are more uncertainties about the exact formation mechanism of the outer Solar System (Goldreich et al. 2004; Helled and Bodenheimer 2014), but there are several lines of evidence to suggest that giant impacts were also a feature of the more distant reaches of the Solar System (e.g., Safronov 1972; Canup 2005). There is also growing evidence for giant impacts having occurred recently in some extrasolar planetary systems, from observations of what could be impact-generated debris (Song et al. 2005; Rhee et al. 2008). Stars with anomalously high levels of dust in their regions that would be analogous to the location of terrestrial planets in the inner Solar System are often interpreted within the context of terrestrial planet formation (e.g., Lisse et al. 2008; Melis et al. 2010), particularly if they are at an age at which planet formation models predict such giant impacts to be taking place (i.e., $\ll 100$ Myr). Clearly, studying this debris and how frequently it is detected around nearby stars has the potential to inform about terrestrial planet formation processes

more generally, as well as the fraction of stars that host such planets (Jackson and Wyatt 2012). Some stars also show evidence that could point to recent giant impacts in the more distant reaches of their planetary systems (Telesco et al. 2005; Dent et al. 2014; Stark et al. 2014), but conclusions remain tentative for now.

The aim of this chapter is to review the topic of giant impacts, focussing on the potential of observations of giant impact debris to inform on planet formation processes. It starts with evidence for giant impacts in the Solar System (Sect. 2) before discussing the various possible observable consequences of such impacts in extrasolar systems (Sect. 3). Generic aspects of the evolution of impact-generated debris are then discussed in Sect. 4. The observability of debris from the Moon-forming giant impact is considered in Sect. 5 and then compared with observations of extrasolar debris disks (Sect. 6). Giant impacts at larger distances from the star are discussed in Sect. 7, followed by a discussion of the implications from debris observations for the formation of the ubiquitous super-Earth class of planetary system (Sect. 8). Conclusions are given in Sect. 9.

2 Giant Impacts in the Solar System

In discussing the role of giant impacts in the formation of planets it is beneficial to turn first to our own Solar System, as here we have detailed information about the final end products—the planets and satellites themselves. Aside from Jupiter and possibly Saturn, true twins for the Solar System planets (in both size and orbital location) remain tantalisingly outside detection limits of searches for extrasolar planets at present. While future missions will certainly extend these detection limits and allow us to begin detecting true Solar System twins, we will presumably always have more information about our own backyard than other star systems. As is common in discussions of planet formation we divide our overview of the evidence for giant impacts in the Solar System into the inner Solar System (interior to Jupiter) and the outer Solar System (exterior to and including Jupiter).

2.1 Inner Solar System

The inner Solar System is replete with evidence for giant impacts. Each of the terrestrial planets has features for which a giant impact explanation has been suggested, with the exception of Venus, and it is probably no coincidence that Venus is also the terrestrial planet whose surface and geological history are least well understood.

Mercury In comparison with the other terrestrial planets Mercury is unusually rich in iron, with a very large core. This extreme iron enrichment can be reproduced by a collision between a roughly 2.25 $M_{\rm Mercury}$ chondritic composition proto-Mercury and a roughly 0.4 $M_{\rm Mercury}$ impactor at speeds of around 30 $\rm km\,s^{-1}$ (e.g. Benz et al. 1988; Cameron et al. 1988; Anic 2006; Benz et al. 2007). This impact speed is around 6 times the escape velocity of proto-Mercury and the resulting impact is extremely violent, almost destroying the planet. While commonly thought of as a 'mantle-stripping' event, in physical terms it is gravitational re-accumulation that is responsible for bringing the core of the former planet back together, rather than the outer layers being peeled away to reveal the exposed core. It is also notable that proto-Mercury in this scenario is very similar in mass to Mars, being around 16 per cent more massive.

Debris is a key component of the formation of Mercury via a giant impact, accounting for a larger fraction of the initial mass than the final planet. As noted by Gladman and Coffey (2009) the fate of this debris, and in particular the fraction that is re-accreted, is essential to the final success or failure of a giant impact model to reproduce Mercury.

Earth-Moon System Perhaps the most striking thing about Earth (from a dynamical perspective) is the large mass of the Moon. At 1.2 per cent of Earth's mass the Moon is, by a substantial margin, the largest satellite relative to the size of its parent planet in the Solar System.

To find a comparable system one must look to the dwarf planet binary Pluto-Charon with a mass ratio of 0.12, and which is also believed to be the result of a giant impact (Sect. 2.2). The angular momentum of the Earth-Moon system is also unusually high—equivalent to a 4 hour rotation period in an isolated Earth, much faster than the other terrestrial planets. Meanwhile tracing back the tidal evolution of the Moon suggests that it would have been much closer to Earth in the early Solar System, and compositionally the Moon is substantially depleted in both iron and volatile elements relative to Earth.

All of these factors led to the suggestion that the Moon might be the product of a giant impact between proto-Earth and another body (e.g. Cameron and Ward 1976; Canup 2004a). Continued work on the giant impact hypothesis eventually resulted in what has become known as the Canonical model (e.g. Canup and Asphaug 2001; Canup 2004a,b), in which a roughly Mars mass body (known as Theia) collides with a nearly fully formed proto-Earth at an oblique angle of $\sim 45^\circ$ and a speed near the mutual escape velocity. Such impacts would have been quite common in the late stages of terrestrial planet formation (e.g. Agnor et al. 1999), and the Canonical model is very successful at reproducing many aspects of the Earth-Moon system.

In recent years the Canonical model has faced something of a crisis in the near indistinguishability of Earth and Moon in isotope ratios, which has spawned a re-think of the giant impact scenario (Asphaug 2014). Some have invoked the evection resonance to permit the Moon to be created with collision parameters that are quite different to the Canonical model, satisfying both the dynamical and isotopic constraints (e.g. Canup 2012; Ćuk and Stewart 2012; Reufer et al. 2012), while others have argued that the Canonical model parameters still satisfy the isotopic constraints, e.g., if some equilibration of the accreted material occurs in the protolunar disk (Pahlevan and Stevenson 2007; Salmon and Canup 2012) or if the impactor formed sufficiently close to the Earth (Mastrobuono-Battisti et al. 2015), but the basic idea of the origin of the Moon in a giant impact does not seem to be in doubt.

Martian Hemispheric Dichotomy The largest topographic feature on Mars is the difference in elevation by $\sim$5 km between the lower northern and higher southern hemispheres (e.g. Smith et al. 1999) commonly referred to as the hemispheric dichotomy. The possibility of the northern lowlands representing a massive impact basin was first suggested by Wilhelms and Squyres (1984). With more recent work (e.g. Andrews-Hanna et al. 2008; Nimmo et al. 2008; Marinova et al. 2008, 2011) this suggestion has become more concrete, and a giant impact appears to be the best explanation for the hemispheric dichotomy.

A giant impact is also suggested as a possible origin for the Martian moons Phobos and Deimos (e.g. Rosenblatt 2011; Rosenblatt and Charnoz 2012; Citron et al. 2015). The Borealis basin impact might thus be responsible for both the hemispheric dichotomy and the formation of the Martian moons.

Asteroid Families and (4) Vesta The Hirayama asteroid families are the result of large collisions within the asteroid belt (e.g. Durda et al. 2007). Though material strength begins to play an important role in asteroid sized bodies large impacts between asteroids share many of the features of giant impacts between planetary bodies (e.g. Jutzi 2015). In the case of (4) Vesta and the associated Vesta family asteroids there is particularly strong link. The second largest asteroid (mean diameter 525 km), Vesta is believed to be differentiated and

possess a largely intact crust, and has been suggested as an intact proto-planet, or even 'the smallest terrestrial planet' (e.g. Keil 2002; Russell et al. 2012). In addition the numerous Vesta family asteroids can be traced to the formation of the massive Rheasilvia basin, which together with the underlying Veneneia basin dominate the southern hemisphere of Vesta. Models of the formation of Rheasilvia indicate a $\sim$66 km diameter impactor (Jutzi et al. 2013). The formation of the Rheasilvia basin can thus be thought of in some senses as a recent ($\lesssim$1 Gyr ago, Binzel et al. e.g. 1997) 'mini' giant impact.

2.2 Outer Solar System

Pluto-Charon As mentioned above the Pluto-Charon system is the closest analogue to the Earth-Moon system, despite lying on average over 40 times further from the Sun and having a substantially different composition, being rich in icy material. Pluto-Charon is well described as a binary, having a mass ratio of around 8.5:1, both bodies being tidally locked to one another, and with the system barycentre lying outside Pluto. The angular momentum in the Pluto-Charon system is larger than could be contained in a single body, suggesting a collisional origin (e.g. McKinnon 1989) and Canup (2005) showed that a giant impact is indeed a good explanation for the Pluto-Charon binary. The smaller satellites in the Pluto-Charon system may also have formed in the giant impact that produced Charon (e.g. Canup 2011), but explaining the complex resonant structure of the small satellites presents some difficulties (e.g. Showalter and Hamilton 2015).

Haumea Collisional Family Analogous to the Hirayama families in the asteroid belt there is presently one collisional family known in the Kuiper belt, that associated with the dwarf planet Haumea (Brown et al. 2007). This collisional family has a significantly lower velocity dispersion than the escape velocity of Haumea, and it has thus been suggested that the collisional family may have been created in an impact with a precursor of the current two satellites of Haumea (Schlichting and Sari 2009; Ćuk et al. 2013) rather than Haumea itself.

Middle-Sized Moons of Saturn It has been suggested that the formation of satellites around the gas giant planets is in many ways like a miniature version of the formation of the Solar System (Canup and Ward 2002, 2006). This would include giant impacts between proto-satellites, and such impacts may explain the origin of the otherwise mysterious middle-sized moons (those $\sim$500–1500 km in diameter) of Saturn (Sekine and Genda 2012; Asphaug and Reufer 2013). In this scenario Saturn would have started out with a system of larger satellites like the Galilean moons of Jupiter, but whereas in the Jovian system these moons remained locked in a stable Laplace resonance, in the Saturnian system they became unstable and collided, with the present middle-sized moons representing the remnants of this former satellite population.

Obliquity of Uranus One of the important features of both the Earth-Moon and Pluto-Charon systems that is well explained by a giant impact scenario is their large angular momentum. Given the large amount of angular momentum that can be imparted by a giant impact, if the impact orientation is substantially different to the spin axis of the planet it is possible for the impact to lead to a large change in the planet's obliquity. It has long been recognised that an impact, involving an impactor around the size of Earth, represents a possible explanation for the large obliquity of Uranus (e.g. Safronov 1972; Parisi and Brunini 1997). An impact is not the only means by which Uranus can be tilted; tidal evolution of a massive retrograde satellite has also been proposed (Greenberg 1974; Kubo-Oka and Nakazawa 1995), though the moon required would have had to be greater than 1.5 times the mass of Mars and thus within an order of magnitude of the mass of proposed impactors.

3 Giant Impact Extrasolar Observables

One conclusion from Sect. 2 is that there is abundant evidence for giant impacts occurring in the Solar System. Indeed, the majority of the planets show some evidence for giant impacts. It is also the case that evidence for the impacts is manifested in many different ways, in terms of the physical or dynamical properties of the planets and their environments. The various consequences of giant impacts are summarised in Table 1, along with the evidence in the Solar System for these outcomes and the potential for observing them in extrasolar systems which is discussed further below.

The formation of moons is one of the most obvious lines of evidence for giant impacts, since this has emerged as the favoured explanation for our own Moon, with other Solar System moons also explained in this way. Given the small mass of any extrasolar moon, it seems like an impossible task to identify them. However, planets as small as 0.066 $M_\oplus$ have been detected in orbit around nearby stars (Jontof-Hutter et al. 2015). The mechanism to find such low mass planets involves looking for small perturbations to the timing of the transit of another large planet in front of the star due to the dynamical perturbation of the smaller object (so-called transit timing variations, or *TTV*s). This may be the most promising way of detecting extrasolar moons, although none are known yet (Kipping et al. 2014). The formation of a moon through giant impact requires an intermediate stage of a circumplanetary disk. There may be evidence for the passage of a circumplanetary ring system in front of its host star 1SWASP J140747.93-394542.6 (Mamajek et al. 2012; Kenworthy and Mamajek 2015). While the nature of that object remains unsure, this may provide evidence for satellite formation processes similar to those discussed in Sect. 2.2 for Saturn's moons. The thermal emission from circumplanetary disks may also enhance the brightness of an extrasolar planet, as has been suggested as the explanation for the spectrum of the Fomalhaut-b planet (Kalas et al. 2013), and it is suggested that rings may also be detectable in transit observations (Zuluaga et al. 2015).

A moon is not always an outcome of a giant impact, since in some cases very little material is placed into orbit around the planet, one example being the loss of Mercury's mantle in a violent collision to leave a high density planet (Sect. 2.1). The number of extrasolar planets for which densities have been measured has increased dramatically recently due to

Table 1 Summary of the consequences of a planetary system being subjected to giant impacts: the evidence for this from the Solar System and the possible manifestation in the observable properties of extrasolar systems

What do giant impacts do?	Evidence in Solar System	Potential extrasolar observable
Formation of moons	Earth-Moon, Pluto-Charon, Saturn?	Transit timing variations from exomoons
Modify internal composition	Mercury's Fe-rich composition	Exoplanet densities inferred from radial velocities and transits
Modify planet surface and atmosphere	Mars' hemispheric dichotomy, past magma ocean	Surface effects subtle, but hot planet spectrum
Modify planet spin	Uranus tilt	Exoplanet spins are measurable
Create debris	Hirayama asteroid families; dust bands; craters on small bodies	Infrared signature

the combination of high sensitivity transit observations with Kepler (that measure the size of the planet) and radial velocity observations (that determine the mass of the planet). In some cases the transit measurements also determine the mass of the planet, providing there are nearby planets from which to measure the TTVs as mentioned above. Such densities are used to infer the composition of the planets, with densities possibly as high as 14 g/cm^3 being recorded (Marcy et al. 2014). This is a promising avenue, but one which has yet to be used to infer a collisional history for the planets, rather this information has been used to assess the presence or absence of an atmosphere.

The effect on the planetary surface is more subtle. For example, the Martian hemispheric dichotomy is only apparent to us because its surface height has been measured at high precision; the level of difference is 0.07 % the diameter of Mars. Variations in surface height may be measured from the shape of the transit of an exoplanet, but the precision required is beyond current instrumentation. However, if the collision is energetic enough, the surface would be melted in the collision resulting in a magma ocean at 1000–3000 K for rocky planets. This molten surface would only be temporary since the heat would be radiated away (e.g., Earth's magma ocean may have survived 2 Myr; Zahnle et al. 2007), but could have a dramatic effect on the emission spectrum of the planet. Whether the hot surface itself is observable depends on the planet's atmospheric properties, which would in turn be modified by the impact; e.g., the early nebula atmosphere could be stripped by impacts (Schlichting et al. 2015; Inamdar and Schlichting 2015), and the atmosphere could also be replenished by magma ocean outgassing. However, it is clear that the excess energy must be radiated somehow, and this can increase the detectability of the planets following impacts (Miller-Ricci et al. 2009; Lupu et al. 2014). Such impact afterglows would be easier to detect at larger distance from the star due to favourable contrast with the stellar emission. This lead to the suggestion that the companion found at 55 au from 2M1207 was in fact the result of an impact between a 7 $M_\oplus$ and 74 $M_\oplus$ planets (Mamajek and Meyer 2007). While more detailed analysis shows that the properties of this system are better explained by the atmospheric properties of a low mass companion without any collision required (Barman et al. 2011), this at least demonstrates that impact afterglows are in the realm of current observational capabilities.

Conservation of angular momentum requires a planet's spin to be modified as a result of a giant impact. In some cases this can be significant, perhaps explaining the tilt of Uranus' spin relative to its orbital plane. Exoplanet spins are already measurable in observations of the velocity profile from lines in their atmospheres (Snellen et al. 2014). For now such observations have been applied to one of the most massive known extrasolar planets ($\sim 8 M_{\rm jup}$ β Pic-b), showing it to spin much faster than its Solar System counterparts, likely due to its higher mass as opposed to its collisional history. There are also prospects to measure the orientation of an exoplanet's spin axis with respect to its orbital plane using observations of its radial velocity during secondary eclipse in a manner analogous to the Rossiter-McLaughlin effect (Nikolov and Sainsbury-Martinez 2015).

It is a general outcome of a collision that some fraction of the mass of the two bodies does not remain bound to either one at the end of this process. Indeed, the loss of Mercury's mantle in a giant collision not only modified the composition of that planet, but also released large quantities of debris. That debris, made up of solid material ranging in size from μm-sized dust grains to km-sized planetesimals, as well as vaporised rock if the collision was energetic enough, ended up orbiting the Sun. There is abundant evidence for the creation of debris in collisions in the asteroid belt, ranging from witnessing dust released in an impact which occurred in the last few years (Jewitt et al. 2011), to clustering in asteroid orbital elements showing these to have been created in an event a few Myr in the past (Nesvorný

et al. 2002), evidence for which is also present in the dust bands in the inner Solar System (Grogan et al. 2001), to the Hirayama asteroid families which may have been much more violent events Gyr-ago (Hirayama 1918). Evidence for debris released in the giant impacts proposed to have shaped the Solar System's planets is harder to find since these collisions likely occurred long ago, shortly after the Solar System formed. Nevertheless such evidence may exist in the cratering record and chemical composition of asteroids and meteorites (Bottke et al. 2015).

From an extrasolar perspective, giant impact debris is expected to be readily detectable, because even relatively small quantities of dust (e.g., that corresponding to an asteroid of a few 10s of km in diameter ground into μm-sized dust) can be detected around nearby stars due to its thermal emission. The dust is heated by the star and then re-radiates that emission in the infrared at levels that can exceed the star's own photospheric flux (Wyatt 2008). Some 20 % of nearby stars show evidence for circumstellar dust originating in the break-up of planetesimals. While a large fraction of this dust is likely produced in the steady state grinding down of extrasolar analogues to the Kuiper belt, since such an interpretation explains the statistics of disk detection as a function of age (Wyatt et al. 2007b), some fraction of these may instead be the signature of a recent giant impact, since giant impact debris is expected to emit at potentially detectable levels (e.g., Jackson and Wyatt 2012).

To summarise, there are many ways in which evidence for giant impacts may be found in extrasolar systems. While there has been much progress in identifying these signatures, for now the most promising evidence for giant impacts in extrasolar systems lies in the creation of debris, and it is to this aspect that the remainder of this chapter will be devoted.

4 Evolution of Debris from Giant Impacts

As noted in Sect. 3, one of the key observable features produced by a giant impact around another star is debris. Though the character of the observable features will vary somewhat depending on the nature of the impact, for example the mass of the colliding bodies, or the orbital distance at which the impact occurs, the underlying processes which shape these features and how they evolve possess many similarities. Here we briefly outline a general framework within which the evolution of giant impact debris may be understood (for a more detailed discussion see Jackson et al. 2014).

4.1 Dynamics of Giant Impact Debris

The dynamical evolution of debris released in a giant impact can be considered as beginning from a single point with velocities relative to the star given by the progenitor's Keplerian orbital velocity v_k plus some velocity dispersion. While the velocity dispersion is likely to be asymmetric, it is convenient to model this as isotropic given that the orientation of any asymmetry would be specific to a given impact, and is likely to be random. The velocity dispersion of debris in giant impact simulations is approximately Gaussian with a width of σ_v (e.g. Jackson and Wyatt 2012), where σ_v is comparable to the escape velocity of the progenitor v_{esc}. The subsequent dynamical evolution and morphology of the debris depends on the ratio σ_v/v_k which is shown in Fig. 1 for different progenitors as a function of orbital distance, using the assumption that $\sigma_v \approx 0.46 v_{esc}$ as found for the Moon-forming impact (Jackson and Wyatt 2012). Note that the velocities of the debris being comparable to the escape velocity of the progenitor (regardless of the progenitor mass) holds largely independently of the velocity distribution of the debris particles. This is because to go into

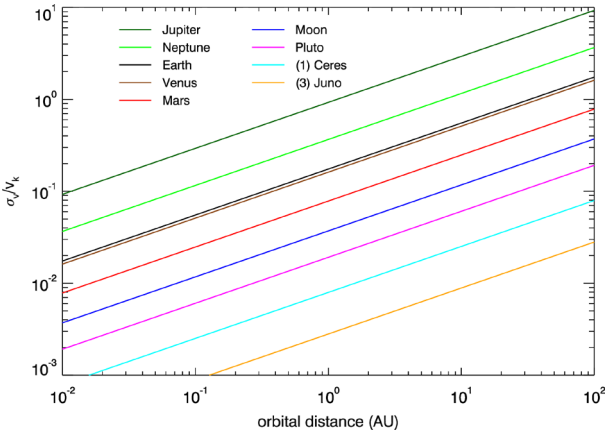

Fig. 1 The scaled velocity dispersion imparted to giant impact debris, σ_v/v_k, as a function of orbital distance of the progenitor for a selection of Solar System bodies ranging in mass from Neptune to the asteroid (3) Juno, under the assumption that $\sigma_v = 0.46 v_{esc}$. This ratio is important for the morphology and subsequent evolution of the debris; e.g., much of the debris may be placed onto orbits that are unbound from the star if $\sigma_v/v_k \gg 1$

heliocentric orbit the debris must have sufficient energy to escape the progenitor body, and once the energy required to escape is exceeded the resulting relative speed post-escape then rapidly becomes comparable to the escape velocity. For example a particle that exceeds the escape velocity by only 5 % at launch will then have a relative speed post-escape of $0.32 v_{esc}$.

To understand the evolution and morphology of the debris it is important to remember that immediately after the impact the debris occupies what is essentially, on the scale of the wider planetary system, a single point at the location of the impact, which we will refer to as the *collision-point* (Jackson and Wyatt 2012; Jackson et al. 2014). This geometry means that the orbits of all debris fragments must pass through this point, which thus has a high density. A small density enhancement is also found on the opposite side of the star from the collision-point, since all debris orbits must pass through the plane of the progenitors' orbit somewhere along what we will refer to as the *anti-collision line* (Jackson and Wyatt 2012; Jackson et al. 2014). Since debris passes through the collision-point once per orbit, the resulting repeat encounters can also have implications for the rate at which debris encounters the progenitor and indeed other debris.

Common to the dynamical evolution of all (bound) giant impact debris are four key morphological phases: (i) After the impact, both the debris and the progenitor move away from the collision-point. The debris initially forms an expanding clump that moves with the progenitor body around its orbit (see upper left panel of Fig. 2). (ii) Since fragments that have been placed onto orbits with smaller semi-major axes than the progenitor will have shorter orbital periods than those with larger semi-major axes, the clump will be sheared as it continues around the orbit. Once the shearing has progressed enough that fragments on smaller orbits have reached the collision-point before those on larger orbits have left it, the clump will become a spiral structure, which then continues to coil as Keplerian shearing continues (see upper right panel of Fig. 2). (iii) Eventually the spiral structure of the debris is no longer visible and the debris forms a smooth but highly asymmetric disk, with a strong pinch at the collision-point (see bottom left panel of Fig. 2). The density enhancement at the collision-point, as well as how spread out the disk is away from the collision-point, both increase with velocity dispersion (i.e., with σ_v/v_k, for more detail see Jackson et al. 2014). (iv) The orbits of debris fragments precess due to interactions with massive bodies, including the progenitor, at a rate that depends on the semi-major axis of the fragments. The resulting differential precession eventually smears out the asymmetry producing an axisymmetric disk (see bottom right panel of Fig. 2).

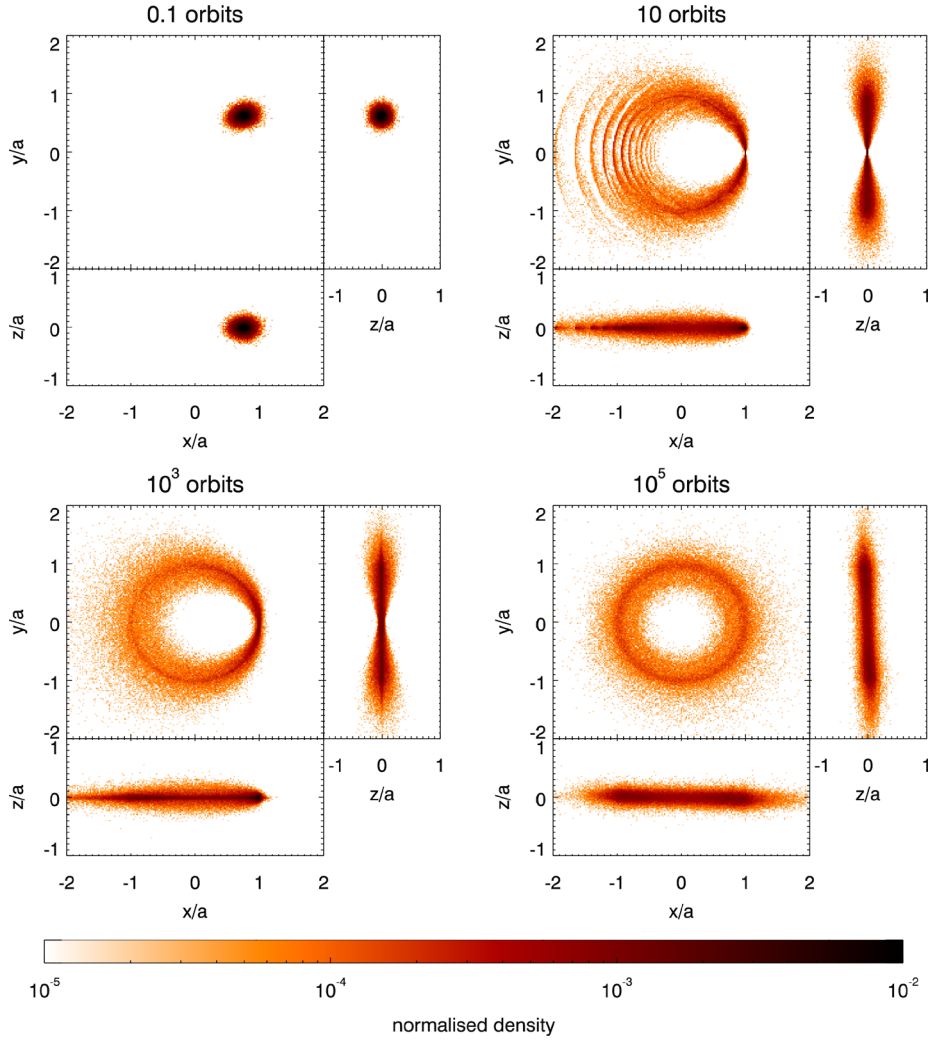

Fig. 2 Snapshots of the distribution of debris ejected by a giant impact with $\sigma_v/v_k = 0.18$, showing the four key stages of its dynamical evolution: (*top left*) clump, (*top right*) spiral, (*bottom left*) asymmetric disk and (*bottom right*) axisymmetric disk. For each stage the *top left panel* shows a face-on view of the disk with the star at the origin and the collision-point at $(1, 0)$, while the *panels to the right and below* this show edge-on views. The axis scale is in units of the progenitor semi-major axis, a, while the snapshot times are in units of the progenitor's orbital period. The *colour* corresponds to the disk density normalised to an integrated value of 1 at time zero

The timescale for the shearing process, and so for the evolution from clump to asymmetric disk, depends on σ_v/v_k. The shearing is quite rapid in Fig. 2 since $\sigma_v/v_k = 0.18$; the early spiral stage is visible after 1 progenitor orbit, and after 100 orbits the spiral is no longer distinguishable. In the case of an impact with a smaller σ_v/v_k the rate of Keplerian shearing is slower, since the velocity difference across the debris distribution is smaller. While this would result in slightly longer clump and spiral phases, in general the clump phase is expected to end within ten orbits, and the spiral phase within a few hundred orbits after the

impact. Since the morphology of the disk, and the rate at which the disk progresses through the early phases of the evolution, depend on σ_v/v_k, this means that impacts involving progenitors of the same mass can have substantially different morphologies and different early stage evolution if they occur at different orbital distances (see Fig. 1).

The smooth asymmetric phase lasts much longer, since it is determined by the precession timescale, rather than by the dynamical timescales that set the clump and spiral phases. Precession rates depend on the system architecture, i.e., the masses and orbits of other planets in the system, although the progenitor itself may also be massive enough to set the precession period. In general the collision-point may be expected to have been smeared out after a few thousand orbits and the disk to have achieved total axisymmetry after a few tens of thousands of orbits, timescales that apply to precession due to a Jupiter mass planet 5 times more distant than the impact (see Eq. 23 of Jackson et al. 2014), or due to an Earth-mass progenitor (Jackson and Wyatt 2012).

The morphological evolution shown in Fig. 2 will occur whatever the wider architecture of the planetary system in which the progenitor and debris reside. However, the progenitor and other planets play a potentially much more important role beyond setting the precession timescale of the debris, since close debris-planet approaches can lead to the debris being accreted onto the planet or ejected from the system. Which of these outcomes is more likely depends on the ratio of the escape velocity of the planet to its Keplerian velocity, v_{esc}/v_k: ejection is more likely for $v_{esc}/v_k \gg 1$ and accretion more likely for $v_{esc}/v_k \ll 1$ (see Fig. 1). The rate at which debris is accreted onto a planet of radius R_p can be estimated as

$$R_{col} = n\sigma_{col}v_{rel}, \tag{1}$$

where n is the density of debris in the vicinity of the planet, v_{rel} is the relative velocity of encounters between the planet and the debris, and $\sigma_{col} = \pi R_p^2[1 + (v_{esc}/v_{rel})^2]$ is the collision cross-section.[1] However, note that this rate may be significantly underestimated at early times for re-accretion onto the progenitor if the geometrical effect of the collision-point is not taken into account; during the early phases of dynamical evolution, most re-accretion onto the progenitor will occur when it passes through the collision-point, and the accretion rate will be substantially raised during this early period (Jackson and Wyatt 2012, see also discussion in Sect. 4.2).

4.2 Collisional Evolution

In addition to evolving through dynamical interactions with massive bodies in the system, the debris will also evolve as a result of mutual collisions within the debris population. Such collisions lead to the break-up of larger fragments into smaller ones, redistributing mass down the debris size distribution. Eventually the debris is ground down into dust grains that are small enough to be removed by radiation pressure on orbital timescales. The size at which this occurs is called the blow-out size and for dust of density ρ is given approximately by (e.g. Wyatt 2008)

$$D_{bl} = 0.8\left(\frac{L_*}{L_\odot}\right)\left(\frac{M_\odot}{M_*}\right)\left(\frac{2700\ \mathrm{kg\,m^{-3}}}{\rho}\right)\ \mu\mathrm{m}. \tag{2}$$

[1] Note that the gravitational focussing factor for re-accretion onto the progenitor is independent of the progenitor's properties, since v_{rel} scales with σ_v and so v_{esc}. This factor is found to be close to 10 for the Moon-forming giant impact debris.

The rate at which debris fragments collide with each other is determined by an equation that is analogous to Eq. (1). This calculation is complicated by the fact that any given debris particle will interact with particles with a range of sizes, with the outcomes of such collisions ranging from cratering to complete pulverisation. For this reason the collisional evolution of debris populations is often studied numerically (Thébault et al. 2003; Krivov et al. 2005; Bottke et al. 2005). However, this is not necessary to understand what happens, because for most common assumptions about collisional outcomes, once the size distribution has reached steady state it tends to a shape that can be readily calculated (O'Brien and Greenberg 2003; Wyatt et al. 2011). If it can be assumed that the strength of a debris fragment is independent of its size, the size distribution tends to a power law

$$n(D) \propto D^{-\alpha}, \tag{3}$$

where $\alpha = 7/2$. Such a size distribution has most of the mass in the largest objects, while most of its cross-sectional area is in the smallest objects (i.e., those close to the blow-out limit in Eq. (2)).

It is important to understand how both mass and cross-sectional area evolve within the debris distribution. It is the cross-sectional area to which the observations discussed in Sect. 3 are sensitive (Wyatt 2008). However that cross-section resides in small grains that are relatively short-lived, and so must be replenished from the larger debris fragments which make up the majority of the mass and have longer collisional lifetimes. The discussion is simplified if the size distribution has a fixed shape, because this implies that cross-sectional area scales with mass by a constant ratio, though this is only true at all times if the debris size distribution starts with the size distribution it will tend to in steady state. Typically the total mass of debris created in a giant impact is well known. For example, for large bodies (those with $\sigma_v/v_k > 0.1$), impacts generally fall in the hit-and-run or partial accretion/erosion regimes with debris releases of around 3–5 % of the colliding mass (Leinhardt and Stewart 2012; Stewart and Leinhardt 2012). This is because for large σ_v/v_k, the impact speed must be a larger fraction of the orbital speed to push the impact into a violent outcome state. Smaller bodies (those with $\sigma_v/v_k \ll 0.1$) are more likely to undergo violent impacts where debris masses can be a much higher fraction of the colliding mass, but if the impact parameters are fairly well constrained the debris mass can also be determined with reasonable confidence. On the other hand the size distribution is not well constrained, as discussed further in Sect. 5.2. This is unfortunate, as for a fixed mass of giant impact debris, both its cross-sectional area and (as we will see below) the timescale of its evolution, are strongly dependent on the size of object where most of the mass is created.

Nevertheless, the above discussion motivates a simple prescription with which to predict the evolution of cross-sectional area of the giant impact debris. It is only necessary to consider the evolution of the mass, which will deplete due to the dynamical processes discussed in Sect. 4.1, and due to the collisional erosion of the largest fragments. A quick estimate for the rate at which the largest fragments deplete by collisions can be made using Eq. (1) and assuming that all the debris is in fragments of the same size. While more accurate calculations are readily available (see Wyatt et al. 2007a), this illustrates how the collisional depletion rate is proportional to the mass of largest fragments. This leads to the mass remaining constant until the largest objects have come to collisional equilibrium, following which the mass decays inversely with time, with dynamical processes further accelerating the depletion process.

There are several caveats to the above picture. For example, it is known that the strength of a debris fragment is dependent on its size, and the debris size distribution may not be

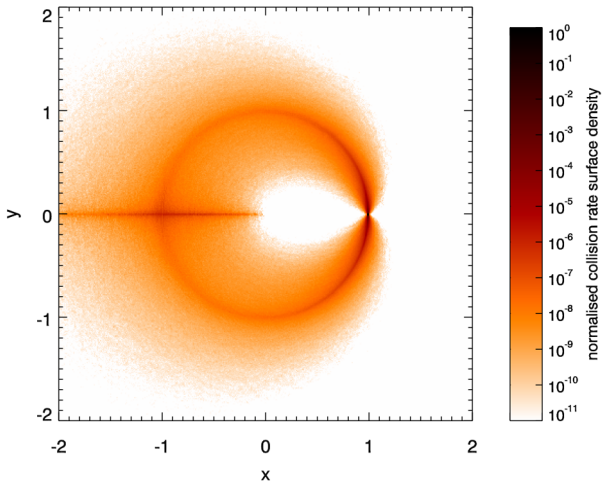

Fig. 3 Image showing how the rate of mutual debris collisions varies with position during the asymmetric phase of evolution of the debris produced by a giant impact with $\sigma_v/v_k = 0.3$. The rates are normalised such that the maximum collision rate is 1. Orbital motion is in the anti-clockwise sense. The geometry of the debris orbits results in an increased density along $y = 0$ (see Fig. 2), and so a higher collision rate at the collision point and along the anti-collision line

expected to start with the shape it tends to in steady state. Both are valid criticisms, but their consequences can be readily accounted for (Löhne et al. 2008; Wyatt et al. 2011). Furthermore, it is found that the simple prescription given above is usually accurate to within a factor of a few and so is acceptable for many applications.

A more complicated caveat to address is the geometrical effect of the collision-point. In the early phases of the dynamical evolution of the disk (prior to axisymmetrisation) the number density varies substantially around the orbits of the debris fragments; in particular the collision-point is a region of exceptionally high density. Figure 3 shows how this results in the collision-point having a collision rate that is many orders of magnitude higher than elsewhere. This effect is such that, to a first approximation, all collisions that a debris particle experiences occur close to the collision-point. It is also such that the collision rate averaged over the particle's orbit is around two orders of magnitude higher than would be the case for an axisymmetric disk; i.e., the rate of collisional evolution will be raised during the early phases of dynamical evolution. The density enhancement along the anti-collision line also leads to a slightly increased collision rate there, though this is much less dramatic. These geometrical effects can only be accounted for using numerical techniques (e.g., Kral et al. 2015), and have further implications which will be discussed in Sect. 7.

5 Observability of Debris from the Moon-Forming Giant Impact

Though recent work has put the Canonical model in some doubt (see Sect. 2.1), the Moon-forming giant impact remains the most well studied example of a giant impact, and thus provides a good starting point for discussions of the behaviour and observability of debris released by giant impacts (for more detail see Jackson and Wyatt 2012).

5.1 Dynamical Evolution

From smoothed-particle hydrodynamics simulations conducted by Marcus et al. (2009) the velocity dispersion of the debris released by the Moon-forming giant impact is well fit by a Gaussian with a width of $\sigma_v = 5.2\,\mathrm{km\,s^{-1}}$. At an orbital distance of 1 au this corresponds to $\sigma_v/v_k = 0.18$ (the value used in Fig. 2). Once it has been launched from Earth the debris goes

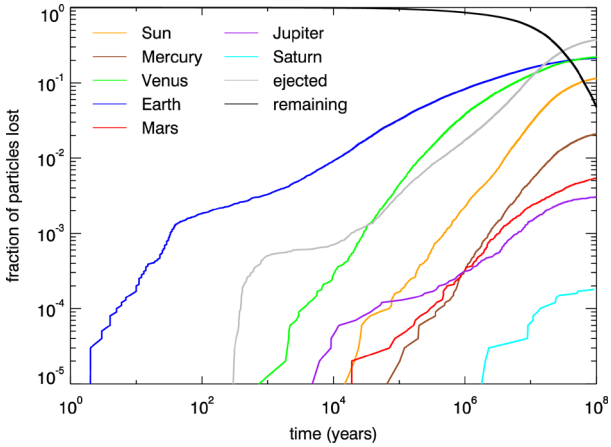

Fig. 4 The fates of particles in a 100 Myr 10^5 particle N-body simulation of debris from the Moon-forming giant impact. Debris particles are massless test particles, and no account is made for collisional erosion. The present day Solar System architecture is used. *Lines for different planets* indicate the fraction of particles accreted onto that planet

into heliocentric orbit and the debris distribution then evolves dynamically as described in Sect. 4.1, with the proviso that the general discussion therein only gave brief consideration to planets in the system other than the progenitor, which were not included in Fig. 2.

The wider architecture of the planetary system becomes important as the giant impact debris leaves the asymmetric stage. The two most important planets aside from Earth in determining the dynamical evolution of the debris are Venus and Jupiter. Venus draws the debris inwards such that, rather than being narrowly peaked around the orbit of Earth, the debris occupies a broad band encompassing the orbits of both Earth and Venus. Jupiter meanwhile truncates the outer edge of the disk by ejecting fragments that encounter it from the Solar System. The differing effects of Venus and Jupiter are in line with expectations from Fig. 1, since Venus has $v_{\rm esc}/v_{\rm k} \ll 1$ while Jupiter has $v_{\rm esc}/v_{\rm k} \gg 1$. Figure 4 shows the ultimate fate of debris created in the Moon-forming impact, which shows that the three fates of accretion by Earth, accretion by Venus, and ejection (mostly by Jupiter) account for the overwhelming majority of the dynamical losses of the debris. The next most likely fate, collision with the Sun, is in fact also a secondary effect of Jupiter; in systems lacking Jupiter the quantity of debris which impacts the Sun is much lower. In total half of the dynamical particles have been lost after 13 Myr, while just 5 % of the dynamical particles remain after 100 Myr.

While of course other planetary systems may have very different orbital architectures to the Solar System, we can expect that some general features of the evolution of the debris from Moon-formation will apply to all systems. In particular we can expect that the most important other bodies in the system will be nearby terrestrial planets of comparable (or larger) mass than the progenitor, and the nearest giant planet. More distant giant planets have limited influence, since the nearest one will almost always eject particles before they have a chance to interact with more distant giant planets (i.e., as long as $v_{\rm esc}/v_{\rm k} \gg 1$).

5.2 Predicted Brightness Evolution

As discussed in Sect. 4.2, the brightness of giant impact debris depends on the quantity of small dust present, which in turn depends on how the debris size distribution evolves due to collisions. Several issues with calculating the collisional evolution were discussed in Sect. 4.2, where it was noted that there may be inherent uncertainties arising from how well the initial size distribution is known, and most collision rate calculations also suffer from

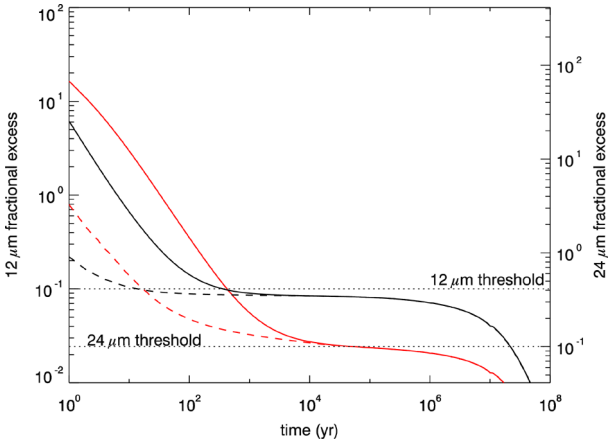

Fig. 5 Evolution of the fractional excess of debris released by a Moon-forming impact around a Sun-like star for different assumptions about its initial size distribution and about its collisional evolution. The fractional excess is defined as the flux from the debris relative to the flux from the stellar photosphere, shown at 12 μm *on the left axis* and 24 μm *on the right axis*; the *dotted lines* show typical detection limits at fractional excesses of 10 % at both wavelengths. The *black lines* show the evolution of a two component size distribution with 30 % vapour condensates up to 1 cm in size and 70 % boulders up to 500 km in size. The *red lines* show the evolution of a three component size distribution with 30 % vapour condensates up to 1 cm in size, 50 % intermediate material up to 7.5 km in size and 20 % large boulders up to 500 km in size. *Solid lines* calculate collision rates assuming the debris to be axisymmetric at all times, while *dashed lines* show the results incorporating some aspects of the collision-point geometry in this calculation (see text for details)

an inaccurate treatment of the geometry of the collision-point. For this reason Fig. 5, which shows the predicted brightness evolution of giant impact debris at two wavelengths 12 and 24 μm at which stars are commonly observed, shows that evolution for two different initial size distributions and two different treatments of the collisional evolution.

There are additional uncertainties involved in translating dust cross-sectional area into the emergent emission spectrum. In all cases on Fig. 5 the emission from the dust is calculated assuming the grains to act like simple blackbodies at the orbital distance of the progenitor. This has the benefit of resulting in a constant ratio between the 12 and 24 μm emission so that both can be shown on the same plot. However, the small grains that dominate the emission are expected to be hotter than black body, while at the same time emitting inefficiently, and potentially exhibiting spectral features due to their composition (e.g., Sect. 6.2). These effects can be properly accounted for, but require additional assumptions (e.g., about the grain composition). For simplicity these are not included in Fig. 5, which should thus be considered to have additional factors of a few or more uncertainty.

As mentioned in Sect. 4.2 the size distribution of debris released by a giant impact is poorly constrained. SPH simulations of giant impacts are unable to resolve anything but the largest debris fragments ($\gg$100 km for Earth-mass impactors; Genda et al. 2015). The main constraint from such simulations is the total mass of the debris, which is around 0.016 $M_{\oplus}$ ($\sim 10^{23}$ kg) in the Canonical model. However, SPH simulations of giant impacts do indicate that, due to the enormous energy involved in the collision of two planetary-sized bodies, a significant fraction of the debris material is released in the form of vapour. As the cloud of vapour expands it cools and condenses, forming small droplets with typical sizes in the mm-cm range (e.g., Melosh and Vickery 1991; Johnson et al. 2012; Johnson and Melosh 2014). For impacts involving Earth-sized bodies, typically a few tens of percent of the debris is released in the form of vapour; Canup (2008) estimated ~10–30 % for the Canonical

Moon-forming impact, though Kraus et al. (2012) suggest that the equations of state in use in current hydrodynamical codes may underestimate vapour production. The production of vapour alongside material that is not vaporised suggests that the size distribution should consist of (at least) two components, the vapour condensates and unvaporised *boulder* material that extends to larger sizes.

The simplest assumption for the initial boulder size distribution is that it starts with the shape it would tend to in steady state (e.g., Eq. (3)) and extends up to some maximum size $D_{\rm max}$. This was the assumption made in Jackson and Wyatt (2012), which is reproduced in Fig. 5 for $D_{\rm max} = 500$ km with the solid black line. This illustrates the properties common to all models for the brightness evolution. In the early phases the vapour condensates shine brightly at readily detectable levels. However, these are rapidly depleted by collisional evolution to non-detectable levels within a few hundred years. Dust arising from the break-up of the boulders starts at a lower level, but is maintained for much longer, eventually starting to deplete after a few Myr due to a combination of collisional erosion and dynamical erosion (see Fig. 4). Taken at face value, the boulder distribution remains undetectable throughout the evolution, and the total emission from both vapour condensates and boulders drops below the typical 12 μm detection threshold after a few hundred years. However, the predicted excess level is so close to the typical detection threshold that, given the various factor of a few uncertainties mentioned elsewhere, the giant impact debris could be detectable at 12 μm up to 10 Myr, which is its duration of detectability at 24 μm.

An alternative choice for the initial size distribution of the boulder material is that of Bottke et al. (2015), basing it instead on the size distribution of the Vesta family asteroids, with additional constraints from Lunar cratering. The size distribution of the Vesta family is considerably steeper than a self-similar cascade, with more mass in smaller bodies.[2] Bottke et al. (2015) suggest that the boulder material may itself have two components, one a steep power law ($\alpha \sim 5$ in Eq. (3)) extending to a largest size of ∼80–100 km and an additional less massive population of larger bodies. The red lines in Fig. 5 show the predicted brightness evolution for a three-component size distribution intended to mimic that of Bottke et al. (2015). The resulting evolution is very similar to that of the two-component distribution considered in Jackson and Wyatt (2012). In particular, it is noticeable that the brightness evolution exhibits just two rather than three distinct phases (i.e., a drop over ∼ 100 years followed by another after ∼ 10 Myr), which is because the emission from the grinding of intermediate-sized (∼ 10 km) material overlaps with the peak from the vapour condensates (since this population is both bright and has a very short collisional lifetime). The relatively low mass in the largest boulders with this assumption makes it less likely that the debris remains detectable up to 10 Myr after the impact event, but any such conclusion would bear the caveat of the factors of few uncertainty in brightness.

The solid lines on Fig. 5 made the same assumption as Jackson and Wyatt (2012) in calculating the collision rate in assuming the debris to be distributed in an axisymmetric torus. The assumption of axisymmetry is common in calculations of collision rates (Wetherill 1967; Wyatt et al. 2010), since precession causes orbits to precess on long timescales. However, in the early phases of evolution the orbital planes and pericentres have yet to be

[2]It is unclear how appropriate it is to extrapolate the Vesta family size distribution to planetary scale giant impacts. For example, the Rheasilvia impact speed of $\sim 15 v_{\rm esc}$ is much faster than typical giant impact speeds, while at ∼0.1 % of the mass of Vesta the 66 km impactor is unusually small (Jutzi et al. 2013). The largest of the Vesta family asteroids (aside from (4) Vesta itself) is only ∼8 km in size, and gravitational re-accumulation may become more efficient at larger sizes. Additionally, the size distribution of Vesta family asteroids may have undergone collisional evolution in the ∼1 Gyr since the Rheasilvia impact. Nevertheless, it may be the only observable example of a giant impact-like debris distribution.

randomised due to precession, and moreover in the clump phase it is incorrect to assume that particles are evenly distributed along their orbits. While such effects are automatically accounted for in the N-body simulations for accretion of debris onto planets, these simulations do not follow debris-debris collisions due to the large number of particles that would be required. It is possible to make a more accurate calculation of the collision rates using the output of the N-body simulations. The dashed lines on Fig. 5 show the evolution using collision rates calculated from the output of the N-body simulations in which the orbital planes and pericentre orientations are no longer assumed to be random (see Fig. 3 and Jackson et al. 2014). As expected from the discussion in Sect. 4.2, the decay in brightness occurs much faster due to the geometry of the collision-point. However, there is a caveat in that this calculation still assumed that particles are evenly spread around their orbits. This means that the collision rate is overestimated during the clump phase, and the true evolution is likely to lie somewhere between the solid and dashed lines on Fig. 5.

A further caveat that applies during the earliest clump and spiral phases is the prospect for the debris to have high optical depth. All of the brightness calculations discussed so far assumed the debris to be optically thin, whereas in fact the dust arising from the break-up of vapour condensates is predicted to be so abundant that its distribution may be optically thick. This could have several consequences, by changing the detectable cross-sectional area, the dust temperature, and whether it is removed from the system by radiation pressure. These effects would also vary on orbital timescales. Clearly further work is needed to improve our understanding of the evolution of giant impact debris during the first tens of orbits. Progress has been made in incorporating collisional evolution into N-body simulations of the evolution of giant impact debris (Kral et al. 2015), however the small volume of the collision-point means that it remains a challenge to accurately model its effect due to the spatial resolution required to do so.

6 Comparison with Observed Systems

6.1 Photometric Fluxes

From Sect. 5.2 it is clear that if we were observing another star shortly after its growing terrestrial planets had undergone an impact similar to that which created the Earth-Moon system, then this event would have had a significant effect on the level of infrared emission observed. Moreover, with multiple such events occurring, it seems that the Solar System would have shone brightly in the mid-IR throughout its infancy. Given the other evidence for collisions occurring throughout the history of the Solar System (see Sect. 2), Rieke et al. (2005) suggested that the scatter in levels of 24 μm emission seen in their Spitzer survey of nearby A stars (i.e., stars slightly more massive and luminous than the Sun), and their higher levels in the first 150 Myr of the stars' lives, could be a result of recent collisions. In that interpretation, high levels of mid-IR emission are attained stochastically following a giant impact, with levels fading back to quiescent levels thereafter. A similar interpretation of 24 μm emission levels was applied to a Spitzer survey of Sun-like stars (Meyer et al. 2008), wherein it was assumed that this emission is indicative of ongoing terrestrial planet formation processes.

However, the situation is complicated, because 24 μm emission can arise for a number of reasons unconnected with collisions or planet formation. It was later shown that both the scatter seen in the Rieke et al. (2005) observations and the decay in emission levels could be explained by the steady state erosion of extrasolar Kuiper belts (Wyatt et al. 2007b); the

level observed simply reflects the initial mass in the belt and its distance from the star, which was far enough that the emission was generally cold and so also explained the observations at 70 μm toward the same stars (Su et al. 2006). The same issue affected the interpretation of Sun-like stars, since it was found that the emission spectrum for the majority of these stars was rising toward longer wavelengths implying that the 24 μm emission arises in a belt far enough from the star (> 10 au) to be explained by steady state processes (Carpenter et al. 2009). That is, while recent giant impacts are not ruled out as the origin of the 24 μm emission, a steady state interpretation is more likely for most systems, and regardless the relatively cool temperature of the emission implies that this arises from a location outside that typically associated with the formation of terrestrial planets.

The problem is simply that while 24 μm emission should accompany a giant impact (see Fig. 5), it is a flawed proxy for such an impact. Nevertheless, the large samples of young stars observed by Spitzer mean that the evolution of a star's (or more accurately a population of stars') 24 μm emission is well characterised (e.g., Siegler et al. 2007), and as such has often been used to assess the frequency of giant impacts (Jackson and Wyatt 2012). More recently it has become clear that a better proxy for such collisions is a star's excess 12 μm emission. Such hot emission is seen less frequently and cannot arise from a more distant Kuiper belt, rather the requisite temperature to emit at such short wavelengths places the dust at a temperature compatible with the location of the terrestrial planets in the Solar System. This does not preclude the presence of a more distant cold dust belt in the system, and indeed there are many examples of debris disks with both cold outer belts and hot inner dust (Su et al. 2013; Kennedy and Wyatt 2014); the hot dust in some of the younger such systems has been attributed to ongoing planet formation processes (Smith et al. 2009a).

Early searches for 12 μm emission from dust around nearby stars with IRAS were not particularly successful (Aumann and Probst 1991), though several good candidates were rediscovered in the last decade and followed up with higher resolution instruments to confirm the emission was associated with the star and to characterise its spectrum (e.g., Rhee et al. 2008; Melis et al. 2010). These hot excesses were picked out on a case-by-case basis, and interpreted again within the context of terrestrial planet formation, based on the fact that the stars with bright emission were predominantly found around < 100 Myr stars.

A significant advance in the statistical analysis of the frequency of stars exhibiting excess 12 μm emission came with WISE, which surveyed the whole sky at that wavelength with a spatial resolution and sensitivity far superior to IRAS. This enabled Kennedy and Wyatt (2013) to quantify the rarity of bright excesses by correlating Sun-like stars in the Hipparcos database with WISE. They found that detectable excesses (those for which 12 μm dust emission is at levels above ~ 10 % that of the stellar photosphere) occur around 1:1000 stars. While it is not feasible to derive the ages of all Hipparcos stars, an age dependence for the excess emission was evident because the majority of the 22 stars with excess were known to be members of young associations. To make a rough estimate of the age dependence, Kennedy and Wyatt (2013) made the assumption that stars in the Hipparcos catalogue have ages that are randomly distributed up to the main sequence age for their spectral type. This led to the conclusion that for stars in the 10–120 Myr age range, the frequency of detectable emission is closer to 3 %; i.e., the excess rate declines with age, just as it does at other wavelengths.

Eventually the WISE data should be mined to determine the excess distributions in all young clusters, similar to the analysis carried out for Spitzer. For now, this has been applied to a few regions such as 10–20 Myr Upper Sco (Luhman and Mamajek 2012) and 3–5 Myr Taurus (Esplin et al. 2014). The interpretation is complicated by the presence of long-lived protoplanetary disk systems among the excess candidates. However, based on this work

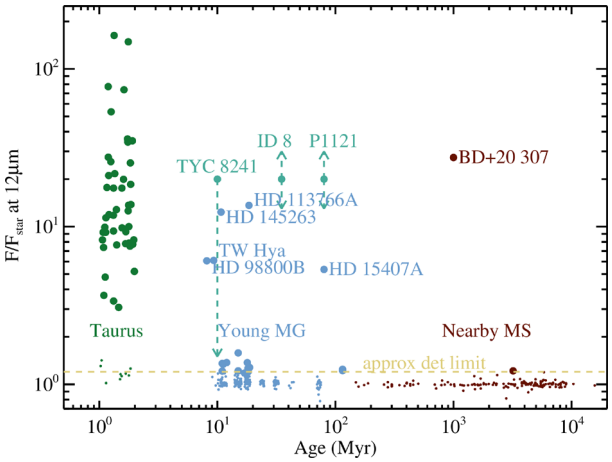

Fig. 6 Evolution of 12 μm emission around Sun-like stars. *Large circles* are those for which an excess above photospheric levels are detected, while *small circles* are those for which no excess is discernable; the approximate detection threshold is given by the *horizontal yellow line*, though this varies from star to star. The *different colours* indicate different surveys: *green* is Taurus (Esplin et al. 2014), *light blue* are young moving groups such as Sco Cen (Rizzuto et al. 2012) and our SED fitting of bona fide members from Malo et al. (2013), *brown* are our SED fits of nearby members from the DEBRIS sample (Phillips et al. 2010). Individually identified 12 μm excess sources are also included from Kennedy and Wyatt (2013). The *vertical dashed lines* show the level of variability for sources discussed in Sect. 6.3 (Melis et al. 2012; Meng et al. 2014, 2015)

we estimate the fraction of Sun-like stars in Upper Sco with detectable 12 μm excesses is ~ 10 %, in broad agreement with the findings of Kennedy and Wyatt (2013), particularly if one considers that the fraction is likely to decrease over the 10–120 Myr age range (and noting that some of the Upper Sco excesses are from protoplanetary disks).

The 12 μm excesses are plotted on Fig. 6 as a function of stellar age for a number of Sun-like stars. Some of these were identified in statistical samples from which the rate of excesses was determined above, but others were simply excess detections reported in the literature such that care should be taken with the interpretation of this plot. Nevertheless, this illustrates the level at which excess is detected, and how that level is typically higher around younger stars. In fact the level of emission around main sequence stars can reach the level seen around T Tauri stars, meaning that the full emission spectrum needs to be considered when interpreting a 12 μm excess, as it is not always clear whether this should be interpreted as evidence for a recent collision or for a protoplanetary disk (Schneider et al. 2013; Kennedy et al. 2014).

6.2 Compositional Constraints

The information provided by a detection of excess emission extends beyond the photometric measurement of the level of excess. For those systems with detections, the mid-IR spectrum provides information about the composition of the dust (e.g., Chen et al. 2006). A prime example of this is the 12 Myr A5V star HD172555 at 29 pc for which the mid-IR spectrum is dominated by emission from amorphous silica dust (Lisse et al. 2009). Dust of different compositions leaves signatures in the spectrum at specific wavelengths; e.g., the silica feature at ~ 9.3 μm allows its presence to be picked out by eye for HD172555. However, extracting more detailed information about the dust composition is not trivial, since the

spectral features are relatively broad so that those from different compositions overlap, and the exact shape of the spectrum depends on the dust size distribution and the temperatures attained by different sizes.

Debris disk modellers commonly employ Mie theory for interpretation of debris disk observations (e.g., Lebreton et al. 2013), however the approximations in this approach mean that such detailed spectra are often interpreted using optical properties obtained from laboratory measurements of astrophysical materials (Lisse et al. 2009). In the case of HD172555 it was the latter approach which was used, resulting in the conclusion that around half of the dust is composed of silica, with a total dust mass equivalent to a 150–200 km asteroid. Since silica is produced in high energy impacts, this points to an origin for the dust in a recent collision at > 10 km/s between two massive protoplanets each at least the mass of Mercury. This interpretation was supported by a feature in the spectrum at 8 μm. While this was originally believed to indicate the presence of SiO gas created in the collision (Lisse et al. 2009), the short lifetime of such gas due to photodissociation suggested an alternative origin for the feature in solid SiO created by condensing vaporised silicate (Johnson et al. 2012). In summary, the composition is similar to that which would have been anticipated following the Earth-Moon forming collision. This analogy is reinforced by the dust temperature which places it at a distance of ~ 6 au from the star, in keeping with spatial constraints from imaging and interferometry (Smith et al. 2012), a location that is comparable in terms of incident energy to the Solar System's terrestrial planets given the higher luminosity of this star.

One puzzling aspect of the dust orbiting HD172555 is its inferred size distribution, since the prominence of the silica feature requires there to be abundant sub-μm dust, whereas such dust is small enough that it would be expected to be blown away from the star by radiation pressure on orbital timescales of a few years (see Eq. (2)). This is in contrast to the persistence of the mid-IR emission at the same level to within 4 % over 27 years (from IRAS to WISE), suggesting that the dust is created more rapidly than it is removed, or that radiation pressure is somehow ineffective. Johnson et al. (2012) preferred the latter explanation, and found that for certain compositions it is possible for this star to retain a long-lived population of $\ll 0.1$ μm grains even if those 0.1–1 μm are significantly depleted; this is because the effect of radiation pressure is strongest for 0.1–1 μm grains, and for certain compositions such grains can have $\beta > 1$ (and so must be unbound) while smaller (and larger) grains have $\beta < 0.5$ (and so can be bound). However, the origin of the size distribution remains unclear, and may be related to the issues discussed in Sect. 6.3, and may also affect the assumed detectability of giant impact debris discussed in Sect. 5.2. Another relevant aspect of this system that we are just beginning to learn about is its gas content; for now it is known that OI is present (Riviere-Marichalar et al. 2012), but its location relative to the hot silica dust is not yet known, as are its origin and impact on the hot dust.

While this section has focussed on just one system, there are many other systems for which compositional constraints exist, not all of which exhibit the same silica composition, even if they are interpreted within the framework of giant collisions (Lisse et al. 2008; Currie et al. 2011; Ballering et al. 2014).

6.3 Time Variability

Whereas the hot dust emission toward HD172555 was concluded to not be variable (see Sect. 6.2), the same is not true for all stars with hot dust mid-IR emission. For example, that of BD+20307 brightened by 7 % over the course of the 6 months between two WISE observations (Kennedy and Wyatt 2013). The case of TYC8241 is particularly interesting,

because the emission persisted at a high level of excess ($\sim$ 10 times brighter than the star at 12 μm) for around 25 years before dropping by an order of magnitude to a negligible level over the course of 2 years (Melis et al. 2012). A good explanation for the disappearance of the hot dust is lacking. One of the ideas proposed is that the dust was removed in a collisional avalanche, a runaway process wherein the input of large quantities of small grains that get blown out by radiation pressure break-up larger debris on their way out (Grigorieva et al. 2007). If so, the previously high levels of excess will return once the population of small dust is replenished in collisions between the bigger debris that was unaffected by the avalanche.

However, given the discussion in Sect. 6.2, perhaps it is not the disappearance of the dust which is surprising, rather it is the earlier persistence of the dust in the face of the star's radiation pressure which is more surprising. Indeed, a two year timescale for the emission to decline is compatible with the orbital removal timescale expected for radiation pressure. The question then would be why radiation pressure was ineffective for so long, and what then caused it to turn on so suddenly?

Another case that is particularly illuminating is that of 35 Myr-old Sun-like (G6V) star ID8 for which the 24 μm emission was noted to be variable in Meng et al. (2012). Later observations showed that the near-IR (3–5 μm) emission to this star underwent a substantial brightening followed by decay on a year timescale, with quasi-periodic modulations (with period $\sim$ 30 days) in the disk flux (Meng et al. 2014). This was interpreted as the result of a giant collision in which silicate vapour is created out of which small particles condense and subsequently collisionally deplete. The geometry of the collision-point during the early phases of the debris evolution explains the periodic modulation (see Sect. 5.1), implying that the collision was located at $\sim$ 0.33 au. Subsequent monitoring of 5 other systems with large levels of mid-IR emission showed that 5/6 of the full sample show significant variations on timescales less than a year (Meng et al. 2015).

Regardless of the origin of this variability, there is an empirical implication for how bright mid-IR emission is interpreted, since its level does not evolve in the manner that the colder dust in debris disks is thought to evolve. That is, the evolution is more complicated than that outlined in Sects. 4.2 and 5.2, in which the dust emission was assumed to decay slowly as the largest objects are ground into dust that is removed by radiation pressure (Eq. (2)). Indeed, the shape of what Kennedy and Wyatt (2013) called the exozodi luminosity function, that is the fraction of stars with 12 μm excess levels above a given level, may already bear witness to that; the luminosity function is relatively flat compared with the expectation that the brightest known excesses will decay due to collisions such that their brightness scales inversely with time.

6.4 How Common Are Late Giant Impacts?

In Jackson and Wyatt (2012) the predicted evolution of 24 μm emission from the debris following the Moon-forming impact was compared with the statistics for nearby stars to estimate the fraction of stars that form terrestrial planets. This section carries out a similar calculation, but for the reasons described in Sect. 6.1 is based on the evolution of the 12 μm emission. The question is also framed slightly differently, so that we seek to determine the fraction of stars that undergo late giant impacts

$$f_{\rm gi} = f_{12} * f_{\rm 12gi}/f_{\rm 12gidet}. \tag{4}$$

That is simply the fraction of 10–120 Myr stars with bright 12 μm excess, f_{12}, multiplied by the fraction of those bright excesses that originate in giant impacts rather than bright asteroid

belts, $f_{12\mathrm{gi}}$, divided by the fraction of the 10–120 Myr timeframe that it would be expected the giant impact debris would be at a detectable level, $f_{12\mathrm{gidet}}$.

One of these parameters is well constrained, since Sect. 6.1 showed that $f_{12} \approx 3$ %, though this may be around a factor of 3 higher at the youngest end of the age range. While $f_{12\mathrm{gi}}$ is not well known, it can be said to be constrained to be less than 100 %. One might be mistaken for thinking that this is close to 100 % from the literature, since mid-IR emission is usually interpreted as the result of giant impacts, but there are not many cases where it is possible to rule out that the dust is simply the bottom end of the collisional cascade of a massive asteroid belt, at least for systems that are in this age range for which collisional processes have yet to have a significant effect on depleting any remnant asteroid belt (Wyatt et al. 2007a).

The hardest parameter to estimate is $f_{12\mathrm{gidet}}$. The most pessimistic assumption would be that there is just one giant impact following the dispersal of the protoplanetary disk (i.e., the Moon-forming impact), and that the dust created from the grinding of boulders is below the detection threshold. This would result in $f_{12\mathrm{gidet}} \approx 10^{-5}$ (i.e., the impact debris is detectable for around 1000 years out of the ~ 100 Myr timeframe). In this case, the only way to explain the high detection rate of 12 μm excesses would be for the majority of these to originate in asteroid belts rather than giant impacts (i.e., $f_{12\mathrm{gi}} < 3 \times 10^{-4}$). However, the conclusion is quite different if the dust from boulders starts out bright enough to be detectable, since the debris from a single impact would remain detectable for ~ 10 Myr, and so $f_{12\mathrm{gidet}} \approx 0.1$. This would mean that $f_{\mathrm{gi}} < 0.3$. This calculation starts to become more constraining if one considers that terrestrial planet formation simulations predict that multiple giant impacts occur in the 10–100 Myr timeframe. Indeed, it is usually assumed that $f_{12\mathrm{gidet}} = 0.5$–1 (Kenyon and Bromley 2004; Jackson and Wyatt 2012; Genda et al. 2015). If this is the case, then the fraction of systems that undergo a late giant impact must be less than 6 %. This would provide a useful constraint for planet formation models, by indicating that either the formation of Solar System-like terrestrial planets is relatively rare, or that planet growth is usually complete by the time the protoplanetary disk disperses; i.e., terrestrial planet formation is not normally accompanied by a late Moon-forming impact, which means planet formation models need to be revised. However, given the caveats on the brightness evolution in Sect. 5.2, strong conclusions cannot yet be drawn.

7 Collisions at Larger Separations

While giant impacts are perhaps most associated with terrestrial planet formation, there is substantial evidence from the Solar System that such events can take place in the outer reaches of planetary systems too (Sect. 2.2). Debris from giant impacts at larger separations undergoes the same evolution as described in Sect. 4. The one point of note is that, for a given progenitor, $\sigma_{\mathrm{v}}/v_{\mathrm{k}}$ will be higher (and so the debris ends up in a broader annulus) for impacts at larger separations (see Fig. 1). However, the considerations for the detectability of debris from large separation impacts are slightly different than for impacts closer to the star (see Jackson et al. 2014).

One obvious difference is that dust is colder at larger separations, and so it is much more difficult to detect its emission at 12 μm. This is compounded by the more general point that a larger mass of dust (and so a larger progenitor mass) is required for a detectable level of emission at larger separations. The emission from giant impact debris at 10s of au would be most readily detected in the far-IR. Cold dust is quite commonly detected around nearby

stars, with ~ 20 % of nearby Sun-like stars having far-IR emission from circumstellar debris (e.g., Eiroa et al. 2013). However, this is not interpreted as giant impact debris. Rather, this dust is believed to be the product of steady state collisional grinding of planetesimal belts that are analogous to the Kuiper Belt in the Solar System (Wyatt et al. 2007b; Löhne et al. 2008; Gáspár et al. 2013). At the large orbital separations inferred for these belts, collisional lifetimes are long enough that their dust can persist several Gyr above the detection threshold. Since observations of how debris levels vary with stellar age are consistent with the collisional erosion of Kuiper belt analogues, this interpretation is favoured over a giant impact origin for the dust (Wyatt et al. 2007b). Thus it is not possible to use the presence of cold dust from photometry to infer a recent giant impact as it was for hot dust found closer to the star (Kenyon and Bromley 2005).

However, as is evident in Fig. 2, the asymmetric morphology of a debris disk may be used to point to a recent giant impact. The detectability of such asymmetries is favoured at large separations, because the orbital timescales there are much longer than those in the terrestrial planet region, which means that the early asymmetric phases of the disk evolution last much longer. For example, while in the terrestrial planet region the typical lifetime of the asymmetric disk is a few thousand years, this lifetime may rise to of order a million years at 10s of au. In addition it is easier to resolve the morphology of debris in the outer reaches of a system due to its larger angular size (notwithstanding the longer wavelength of the emission). The most intuitive evidence of a giant impact would be the detection of an expanding clump (e.g., Wyatt and Dent 2002). However, the clump phase is so short-lived that it is much less likely to be witnessed than the asymmetric disk phase which is much longer lived.

In addition to the asymmetry in the distribution of debris seen in Fig. 2, the dominance of the collision-point in setting the collision rate of the debris means it plays a further important role in enhancing the asymmetry observed during the asymmetric disk phase at wavelengths that trace the distribution of certain collision products. Such products include the very smallest dust grains that are placed on orbits that are significantly modified by radiation pressure (i.e., those close to or below the blow-out limit given by Eq. (2)). This is because such grains are put on orbits with pericentres that are close to the site of their production, which means that when such grains are closest to the star they are predominantly found close to the collision-point (see Fig. 3). This leads to an excess of hot emission at this point, which may stand out further because such grains are also heated to temperatures above black body equilibrium (and so are much hotter than the rest of the debris); their apocentre distribution also means that their spatial distribution extends to much larger distance on the side of the star opposite the collision-point.

Another collision product with an enhanced asymmetry due to the collision-point is carbon monoxide (CO) gas. Cold bodies at large distances from their host star may contain CO ice (e.g., Solar System comets are typically $\sim$1–10 % CO by mass), and when they are broken up in collisions this might be released as gas, promptly through vaporisation of the ice in the collision, or perhaps delayed through desorption from freshly exposed surfaces. CO gas has a comparatively short lifetime of around 150 years to photo-dissociation by interstellar ultraviolet radiation (e.g. Visser et al. 2009). This is comparable to the orbital timescale at tens of au from the host star, and thus the CO will undergo substantial decay over the course of the orbit after its production, which is predominantly at the collision-point (see Fig. 3). Thus the asymmetry in the CO distribution will be enhanced relative to the parent body population, since not only does the disk geometry reduce the CO density away from the collision-point, but so does the photo-dissociation.

One system in which this effect might be visible is the well known edge-on disk of β Pic. Telesco et al. (2005) revealed a large brightness asymmetry in the SW portion of the disk at

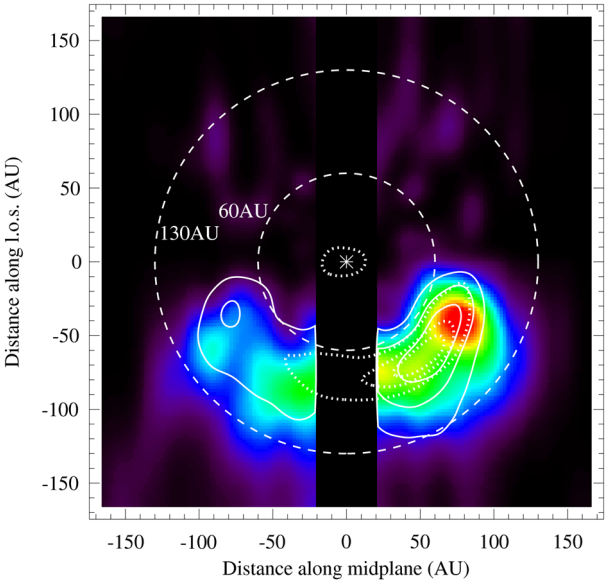

Fig. 7 Image of the face-on distribution of CO gas in the β Pic disk, derived from spatial and velocity information in ALMA observations of this edge-on disk (Dent et al. 2014). Note this is just one possible de-projection, since the observations are insensitive to reflections in the x-axis (i.e., the gas has the same line-of-sight velocity whether it is *in front* or *behind the star*). The *dashed circles* denote the inner and outer radii of the gas disk at 60–130 au, and the *asterisk* represents the location of the star. The distance along the line of sight (l.o.s.) is relative to the stellar position and is positive for gas on the far side of the star; orbital motion is clockwise. Overlaid on the *colour map* of the observed CO are *contours* of a model for CO produced at the collision-point of a giant impact involving Mars-size embryos at 85 au (Jackson et al. 2014). The *solid contours* show the model distribution after being run through the same de-projection process as the ALMA data, while the *dotted contours* show the true distribution

a projected separation of 52 au in the mid-infrared, and Dent et al. (2014) showed that this asymmetry is also present at a lower level in sub-millimetre continuum images. Dent et al. (2014) also found that an asymmetry is present in CO line observations at the same location, but with a significantly greater contrast. The CO line observations also provide information on the line-of-sight velocity of the gas, allowing the edge-on images of the gas distribution to be de-projected to get a face-on view of the disk, under the assumption that the gas is in Keplerian rotation. Figure 7 shows one possible de-projection in which most of the CO is in a clump at around 85 au from the star, with a tail extending 1/3 of an orbit in front of the clump (Dent et al. 2014). In optical scattered light the asymmetry is reversed, with the dust extending around 25 % farther in the NE compared with the SW (Larwood and Kalas 2001).

While it is possible that the clump in β Pic was created in the break-up of a planetesimal within the last 50 years (Telesco et al. 2005), we are many orders of magnitude more likely to witness the same impact in the asymmetric disk phase than in the clump phase. Moreover the morphology, and in particular its wavelength dependence outlined above, are exactly that expected if the asymmetry in the clump is the result of a giant impact witnessed in the asymmetric disk phase; e.g., Fig. 7 shows contours corresponding to a model for CO gas produced in a giant impact onto a Mars-sized progenitor occurring at 85 au from the star (based on the model presented in Jackson et al. 2014). However, an alternative explanation exists for the asymmetry in the β Pic disk that invokes a population of debris trapped in resonance with an unseen planet (Dent et al. 2014). Such resonant populations have a clumpy

distribution (e.g. Wyatt 2003), and the collision rates would be enhanced in the clumps (Wyatt 2006), leading to similar asymmetries in the distributions of both CO and small grains to those of the asymmetric disk phase of a giant impact.

One way to distinguish between the two interpretations is to look for motion of the clump relative to the star, since the collision-point in the giant impact model is stationary on orbital timescales (only moving on much longer precession timescales), whereas resonant clumps would move with the planet. Li et al. (2012) re-imaged the mid-infrared clump and found tentative evidence for motion, but further observations are needed to definitively confirm or reject its motion. If the clump were found to be stationary, and so the giant impact interpretation favoured, this would have significant implications for our understanding of planet formation processes in the outer reaches of planetary systems. This would imply that sufficient Mars-sized embryos exist at a time of ~ 20 Myr after the star formed for us to be likely to witness a collision between them in a ~ 10 Myr timeframe. This would set constraints on the total mass of such embryos and how they are distributed in the disk and could be compared with models for the formation of such embryos (e.g., Kenyon and Bromley 2008). It would also boost the prospects for observing such collisions in other disks, as has been already been proposed for HD181327 (Stark et al. 2014).

8 Giant Collisions in Super-Earth Systems

As pointed out in Sect. 7, while giant impacts are an integral part of the process of forming bodies like our own terrestrial planets, they are not exclusive to the formation of Solar System-like terrestrial planets. One of the most interesting outcomes of exoplanet searches in recent years is the emergence of a new class of *super-Earth* planets. Such planets lie between roughly Earth and Neptune in size and/or mass and orbit in the inner regions of their planetary systems. There are no analogues to these planets in our Solar System, and yet they make up a substantial portion of the population of exoplanets discovered to date, thought to exist around 30–50 % of stars (Howard et al. 2010; Mayor et al. 2011). As such the formation mechanism of these planets is the subject of intense study and debate.

The key question regarding the origin of super-Earths is whether they formed in-situ at $\ll 1$ au (Hansen and Murray 2012, 2013; Chiang and Laughlin 2013) or at larger distance then migrated in through interaction with the protoplanetary disk (Alibert et al. 2006; Lopez et al. 2012; Kenyon and Bromley 2014). Knowing the internal composition of the planets would help, e.g. with a more distant formation location favoured for volatile-rich planets. A significant question is thus whether these planets are 'super-Earths' that are largely rocky, or 'sub-Neptunes' that are rich in volatile elements. It is becoming clear that planets with radii larger than around 1.5 $R_\oplus$ cannot be purely rocky (e.g. Weiss and Marcy 2014; Rogers 2015), however the nature and quantity of the lighter component of planets inferred to have low density is unclear. Planets with radii of around 2–3 $R_\oplus$ can be well fit by a rocky core with a hydrogen-helium envelope that comprises $\sim$0.1–5 per cent of the planet mass (e.g. Wolfgang and Lopez 2015), however they could equally well have less hydrogen and helium, but be predominantly composed of water (e.g. Seager et al. 2007; Howe et al. 2014). Thus far atmospheric studies of such planets have been inconclusive (e.g. Knutson et al. 2014; Kreidberg et al. 2014).

This section explores the possibility that constraints can be set on the origin and evolution of super-Earth planets by considering the debris released in giant impacts involving such planets. If rocky super-Earths form in situ in the same way as smaller terrestrial planets, they would be expected to undergo giant impacts with concomitant debris releases during their

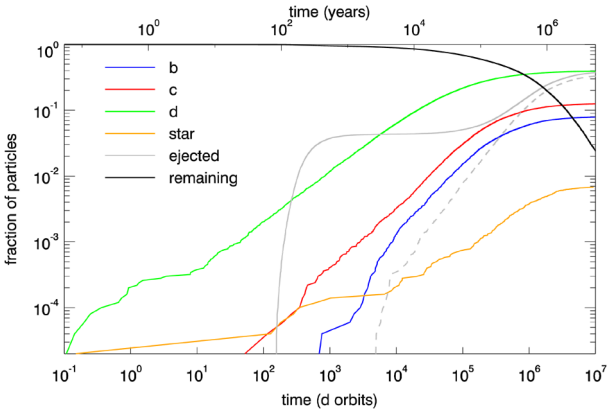

Fig. 8 Fate of particles in a 50000 particle N-body simulation of debris released in a giant impact onto the planet HD 69830d. Time is given in terms of d orbital periods (197 days). By 10^7 d orbits after the impact >95 per cent of the debris has been lost. *Both dashed and solid grey lines* correspond to particles that are ejected, however for the *dashed line* the prompt ejections (i.e., those particles placed on unbound orbits in the impact itself) are removed to make the longer term evolution more visible. The *black line* shows the number of particles remaining in the simulation

formation. A super-Earth planetary system formed by inward migration may also undergo a late phase of giant impacts after the protoplanetary disk dispersed, for example if this promoted instability in the system. Regardless of its origin a super-Earth planetary system may also undergo late giant impacts with any remnant planetary embryos in the system. While the rate of giant impacts experienced by a super-Earth system has yet to be discussed in the literature, the discussion in Sect. 6.4 shows that it should at least be possible to set constraints on that rate from observations.

To focus the discussion of giant impact debris in super-Earth systems, here we consider the HD 69830 system. This system contains three super-Earth planets with minimum masses of 10.2, 11.8 and 18.1 $M_\oplus$ at orbital distances of 0.079, 0.19 and 0.63 au respectively (Lovis et al. 2006) as well as a bright hot debris disk (Beichman et al. 2005). Modelling of the dust emission spectrum suggests that the debris is centred at around 1 au (Lisse et al. 2007), though this indirect constraint on its radial location has a factor of a few uncertainty; direct measurements of the radial location are consistent with a 1 au location, but again have a factor of a few uncertainty (Smith et al. 2009b). This system is particularly interesting as collisional modelling indicates that the dust cannot be produced by the steady-state grinding of a planetesimal belt that has existed at 1 au since the formation of the system ∼2 Gyr ago, but rather must have been created more recently (Wyatt et al. 2007b; Heng and Tremaine 2010). The fact that the predicted location of the debris disk is very close to, and could be coincident with, the outermost planet HD 69830d also points to the possibility that the two are related.

While there are other explanations for the dust that do not involve HD 69830d, such as a recent collision within a stable asteroid belt at 1 au (Wyatt et al. 2010) or a super-comet (Beichman et al. 2005), consideration of giant impact debris from HD 69830d will highlight the differences and similarities to terrestrial planet giant impact debris that will be useful for a more general discussion of the detectability of super-Earth giant impact debris. Figure 8 shows results from a simulation of the dynamical evolution of debris released by a hypothetical impact involving HD 69830d. For the purposes of determining the velocity dispersion of the debris it was assumed that the planet has the same density as Neptune

(1.64 g/cm^3), which leads to $\sigma_v/v_k = 0.32$. This shows that accretion onto all of the planets (b, c and d) is rapid, as is ejection, with around 98 % of the particles having been lost by 10^7 d orbits (5 Myr) after the impact (with roughly twice as many lost to accretion as to ejection). This contrasts with the Solar System case of debris from Moon-formation where only 44 % of the particles had been lost to dynamical effects at 10 Myr (see Fig. 4).

A substantial part of this difference is due to the larger radii of the HD 69830 planets, since a Neptune-like HD 69830d has a radius of almost 4 $R_\oplus$ which would result in an accretion rate 16 times larger than Earth (Eq. (1), noting that re-accretion onto progenitors has a similar gravitational focussing factor). A more Earth-like composition, with a higher bulk density, would result in a smaller radius and a lower accretion rate, and so a longer dynamical evolution than shown in Fig. 8. Another difference with debris from the Moon-forming impact is that the accretion curves of all three planets around HD 69830 are roughly parallel. This is because the larger mass (and escape velocity) of HD 69830d compared with Earth leads to the debris being much more broadly distributed across the system. As a result, and due to the relatively closely-packed nature of the system, all three planets interact strongly with the debris from the beginning of the simulation. A higher density for HD 69830d would enhance this effect due to the corresponding increase in σ_v.

In addition to the more rapid dynamical evolution for super-Earth impact debris, the collisional evolution will also be faster, since the launch (and so collision) velocities will be higher than for debris from an Earth-like planet. A larger fraction of the debris may also be released as vapour, since the larger escape velocities of super-Earths imply that material ejected in their giant impacts will have been subject to more violent shocks. Both of these effects would add to the tendency for debris from a super-Earth giant impact to last for less time than one involving an Earth-size planet. While the initial mass of debris released from a more massive planet will be larger, this cannot offset the more rapid collisional evolution of debris from a super-Earth giant impact and so the duration of detectability would be unaffected, though this would mean that the disk is brighter while it is present.

This section only scratches the surface of the topic of giant impacts in systems of super-Earths. However, it is clear that there are potential implications for our understanding of the formation and composition of these worlds. For example, Eq. (4) can be rewritten as

$$t_{\rm gise12} = 100\ {\rm Myr} * f_{12} * f_{\rm 12gise}/f_{\rm se}, \tag{5}$$

where $f_{\rm se} \approx 0.3$ is the fraction of stars that form super-Earths, $f_{12} \approx 0.03$ is the fraction of 10–120 Myr stars that have 12 μm excess, $f_{\rm 12gise} < 1$ is the fraction of those 12 μm excesses that arise from giant impacts onto super-Earths, and $t_{\rm gise12}$ is the duration of detectability of giant impact debris in the 10–100 Myr window from super-Earths at 12 μm. This calculation benefits from several parameters being well constrained, leading to $t_{\rm gise12} < 10$ Myr. This excludes a long period of late giant impacts which make long-lived detectable debris, which could suggest most of the formation processes takes place in the protoplanetary disk, and/or that only a small fraction of the impact-generated debris is in the form of boulders. However, the 0.06 au radial location of the dust around $\sim$ 60 Myr-old V488 Per was noted to be similar to that of transiting planets discovered by the Kepler satellite (Zuckerman et al. 2012), suggesting a possible origin in super-Earth giant impact debris. If confirmed this could indicate that such debris persists for a non-negligible duration (e.g., $t_{\rm gise12} > 0.1$ Myr).

9 Conclusions

There is abundant evidence for giant impacts in the history of the Solar System. There are many ways in which such impacts could be manifested in observations of extrasolar sys-

tems, including in the properties of any extrasolar planets (e.g., their spin, surface, density, atmosphere, and moons), but the most promising method at the moment for detecting giant impacts is through debris released in the collisions and the resulting infrared emission from dust that is heated by the star. This dust is likely to be readily detectable long after the event, up to 10–40 Myr in the case of the Earth-Moon forming impact. However, there remain significant uncertainties in the duration of detectability because of the unknown size distribution of impact-generated debris.

There are 10s of candidate young Sun-like stars with bright mid-IR emission from dust at levels expected following a giant collision like that which created the Moon. One of the best candidates for giant impact debris is around the star HD172555, since its spectrum shows dust with a silica composition that suggests an origin in a hypervelocity impact. Other systems also show complex variability in their emission, similar to that expected due to the dynamical and physical evolution of impact generated debris, which could provide a valuable window into these events. Despite the growing number of examples of potential giant impact debris, the occurrence rate of such emission is relatively low, at a few %, which either implies that late stage giant impacts are rare (i.e., planet formation is largely complete by the time the protoplanetary disk has dispersed), or that the debris from impacts rapidly grinds itself down to undetectable levels.

Giant impacts in terrestrial planet forming regions are those most readily identified, since these inner regions are usually clear of dust following the dispersal of the protoplanetary disk. However, giant impacts may also occur at larger distances from the stars (at 10s of au). At such distances, larger quantities of debris are required to be detected photometrically, not least because emission from cold debris is relatively common at this distance (~ 20 % for Sun-like stars), so evidence for giant impacts must rest on the morphology of the disk. A clump observed in the β Pictoris debris disk may be evidence of a collision between icy Mars-sized embryos. If so this would require the outer regions of this system to be host to multiple such embryos to give a reasonable chance of witnessing a collision. The ubiquitous class of super-Earth planetary system may also be subject to giant impacts. This chapter provides an initial exploration of this topic by showing how the dynamical evolution differs from that of Moon-forming debris, and it is shown that studying such impacts could provide important clues to the formation of super-Earth systems.

Acknowledgements M.C. Wyatt is grateful for support from the European Union through ERC grant number 279973.

References

C.B. Agnor, R.M. Canup, H.F. Levison, On the character and consequences of large impacts in the late stage of terrestrial planet formation. Icarus **142**, 219–237 (1999)

Y. Alibert, I. Baraffe, W. Benz, G. Chabrier, C. Mordasini, C. Lovis, M. Mayor, F. Pepe, F. Bouchy, D. Queloz, S. Udry, Formation and structure of the three Neptune-mass planets system around HD 69830. Astron. Astrophys. **455**, 25–28 (2006)

J.C. Andrews-Hanna, M.T. Zuber, W.B. Banerdt, The Borealis basin and the origin of the martian crustal dichotomy. Nature **453**, 1212–1215 (2008)

A. Anic, Giant collisions in the early solar system. Ph.D. thesis, Univ. Bern, 2006, http://space.unibe.ch/fileadmin/media/pdf/taps/diss-augustina.pdf

E. Asphaug, Impact origin of the Moon? Annu. Rev. Earth Planet. Sci. **42**, 551–578 (2014)
E. Asphaug, A. Reufer, Late origin of the Saturn system. Icarus **223**, 544–565 (2013)
H.H. Aumann, R.G. Probst, Search for Vega-like nearby stars with 12 micron excess. Astrophys. J. **368**, 264–271 (1991)
N.P. Ballering, G.H. Rieke, A. Gáspár, Probing the terrestrial regions of planetary systems: Warm debris disks with emission features. Astrophys. J. **793**, 57 (2014)
T.S. Barman, B. Macintosh, Q.M. Konopacky, C. Marois, The young planet-mass object 2M1207b: A cool, cloudy, and methane-poor atmosphere. Astrophys. J. Lett. **735**, 39 (2011)
C.A. Beichman, G. Bryden, T.N. Gautier, K.R. Stapelfeldt, M.W. Werner, K. Misselt, G. Rieke, J. Stansberry, D. Trilling, An excess due to small grains around the nearby K0 V Star HD 69830: Asteroid or cometary debris? Astrophys. J. **626**, 1061–1069 (2005)
W. Benz, W.L. Slattery, A.G.W. Cameron, Collisional stripping of Mercury's mantle. Icarus **74**, 516–528 (1988)
W. Benz, A. Anic, J. Horner, J.A. Whitby, The origin of Mercury. Space Sci. Rev. **132**, 189–202 (2007)
R.P. Binzel, M.J. Gaffey, P.C. Thomas, B.H. Zellner, A.D. Storrs, E.N. Wells, Geologic mapping of Vesta from 1994 Hubble space telescope images. Icarus **128**, 95–103 (1997)
W.F. Bottke, D.D. Durda, D. Nesvorný, R. Jedicke, A. Morbidelli, D. Vokrouhlický, H. Levison, The fossilized size distribution of the main asteroid belt. Icarus **175**, 111–140 (2005)
W.F. Bottke, D. Vokrouhlický, S. Marchi, T. Swindle, E.R.D. Scott, J.R. Weirich, H. Levison, Dating the Moon-forming impact event with asteroidal meteorites. Science **348**, 321–323 (2015)
M.E. Brown, K.M. Barkume, D. Ragozzine, E.L. Schaller, A collisional family of icy objects in the Kuiper belt. Nature **446**, 294–296 (2007)
A.G.W. Cameron, W.R. Ward, The origin of the Moon, in *Abstracts of the Lunar and Planetary Science Conference*, vol. 7, 1976, p. 120
A.G.W. Cameron, W. Benz, B. Fegley Jr., W.L. Slattery, The strange density of Mercury—Theoretical considerations, in *Mercury*, ed. by F. Vilas, C.R. Chapman, M.S. Matthews (1988), pp. 692–708
R.M. Canup, Dynamics of lunar formation. Annu. Rev. Astron. Astrophys. **42**, 441–475 (2004a)
R.M. Canup, Simulations of a late lunar-forming impact. Icarus **168**, 433–456 (2004b)
R.M. Canup, A giant impact origin of Pluto-Charon. Science **307**, 546–550 (2005)
R.M. Canup, Lunar-forming collisions with pre-impact rotation. Icarus **196**, 518–538 (2008)
R.M. Canup, On a giant impact origin of Charon, Nix, and Hydra. Astron. J. **141**, 35 (2011)
R.M. Canup, Forming a Moon with an Earth-like composition via a giant impact. Science **338**, 1052 (2012)
R.M. Canup, E. Asphaug, Origin of the Moon in a giant impact near the end of the Earth's formation. Nature **412**, 708–712 (2001)
R.M. Canup, W.R. Ward, Formation of the Galilean satellites: Conditions of accretion. Astron. J. **124**, 3404–3423 (2002)
R.M. Canup, W.R. Ward, A common mass scaling for satellite systems of gaseous planets. Nature **441**, 834–839 (2006)
J.M. Carpenter, J. Bouwman, E.E. Mamajek, M.R. Meyer, L.A. Hillenbrand, D.E. Backman, T. Henning, D.C. Hines, D. Hollenbach, J.S. Kim, A. Moro-Martin, I. Pascucci, M.D. Silverstone, J.R. Stauffer, S. Wolf, Formation and evolution of planetary systems: Properties of debris dust around solar-type stars. Astrophys. J. Suppl. Ser. **181**, 197–226 (2009)
C.H. Chen, B.A. Sargent, C. Bohac, K.H. Kim, E. Leibensperger, M. Jura, J. Najita, W.J. Forrest, D.M. Watson, G.C. Sloan, L.D. Keller, Spitzer IRS spectroscopy of IRAS-discovered debris disks. Astrophys. J. Suppl. Ser. **166**, 351–377 (2006)
E. Chiang, G. Laughlin, The minimum-mass extrasolar nebula: In situ formation of close-in super-Earths. Mon. Not. R. Astron. Soc. **431**, 3444–3455 (2013)
R.I. Citron, H. Genda, S. Ida, Formation of Phobos and Deimos via a giant impact. Icarus **252**, 334–338 (2015)
M. Ćuk, S.T. Stewart, Making the Moon from a fast-spinning Earth: A giant impact followed by resonant despinning. Science **338**, 1047 (2012)
M. Ćuk, D. Ragozzine, D. Nesvorný, On the dynamics and origin of Haumea's Moons. Astron. J. **146**, 89 (2013)
T. Currie, C.M. Lisse, A. Sicilia-Aguilar, G.H. Rieke, K.Y.L. Su, Spitzer infrared spectrograph spectroscopy of the 10 Myr old EF Cha debris disk: Evidence for phyllosilicate-rich dust in the terrestrial zone. Astrophys. J. **734**, 115 (2011)
W.R.F. Dent, M.C. Wyatt, A. Roberge, J.-C. Augereau, S. Casassus, S. Corder, J.S. Greaves, I. de Gregorio-Monsalvo, A. Hales, A.P. Jackson, A.M. Hughes, A.-M. Lagrange, B. Matthews, D. Wilner, Molecular gas clumps from the destruction of icy bodies in the β Pictoris debris disk. Science **343**, 1490–1492 (2014)

D.D. Durda, W.F. Bottke, D. Nesvorný, B.L. Enke, W.J. Merline, E. Asphaug, D.C. Richardson, Size-frequency distributions of fragments from SPH/ N-body simulations of asteroid impacts: Comparison with observed asteroid families. Icarus **186**, 498–516 (2007)

C. Eiroa, J.P. Marshall, A. Mora, B. Montesinos, O. Absil, J.C. Augereau, A. Bayo, G. Bryden, W. Danchi, C. del Burgo, S. Ertel, M. Fridlund, A.M. Heras, A.V. Krivov, R. Launhardt, R. Liseau, T. Löhne, J. Maldonado, G.L. Pilbratt, A. Roberge, J. Rodmann, J. Sanz-Forcada, E. Solano, K. Stapelfeldt, P. Thébault, S. Wolf, D. Ardila, M. Arévalo, C. Beichmann, V. Faramaz, B.M. González-García, R. Gutiérrez, J. Lebreton, R. Martínez-Arnáiz, G. Meeus, D. Montes, G. Olofsson, K.Y.L. Su, G.J. White, D. Barrado, M. Fukagawa, E. Grün, I. Kamp, R. Lorente, A. Morbidelli, S. Müller, H. Mutschke, T. Nakagawa, I. Ribas, H. Walker, DUst around NEarby Stars. The survey observational results. Astron. Astrophys. **555**, 11 (2013)

T.L. Esplin, K.L. Luhman, E.E. Mamajek, A WISE survey of circumstellar disks in Taurus. Astrophys. J. **784**, 126 (2014)

A. Gáspár, G.H. Rieke, Z. Balog, The collisional evolution of debris disks. Astrophys. J. **768**, 25 (2013)

H. Genda, H. Kobayashi, E. Kokubo, Warm debris disks produced by giant impacts during terrestrial planet formation. Astrophys. J. **810**, 136 (2015)

B. Gladman, J. Coffey, Mercurian impact ejecta: Meteorites and mantle. Meteorit. Planet. Sci. **44**, 285–291 (2009)

P. Goldreich, Y. Lithwick, R. Sari, Final stages of planet formation. Astrophys. J. **614**, 497–507 (2004)

R. Greenberg, Outcomes of tidal evolution for orbits with arbitrary inclination. Icarus **23**, 51–58 (1974)

A. Grigorieva, P. Artymowicz, P. Thébault, Collisional dust avalanches in debris discs. Astron. Astrophys. **461**, 537–549 (2007)

K. Grogan, S.F. Dermott, D.D. Durda, The size-frequency distribution of the zodiacal cloud: Evidence from the solar system dust bands. Icarus **152**, 251–267 (2001)

K.E. Haisch Jr., E.A. Lada, C.J. Lada, Disk frequencies and lifetimes in young clusters. Astrophys. J. Lett. **553**, 153–156 (2001)

A.N. Halliday, A young Moon-forming giant impact at 70–110 million years accompanied by late-stage mixing, core formation and degassing of the Earth. Philos. Trans. R. Soc. A, Math. Phys. Eng. Sci. **366**, 4163–4181 (2008)

B.M.S. Hansen, Formation of the terrestrial planets from a narrow annulus. Astrophys. J. **703**, 1131–1140 (2009)

B.M.S. Hansen, N. Murray, Migration then assembly: Formation of Neptune-mass planets inside 1 AU. Astrophys. J. **751**, 158 (2012)

B.M.S. Hansen, N. Murray, Testing in situ assembly with the Kepler planet candidate sample. Astrophys. J. **775**, 53 (2013)

R. Helled, P. Bodenheimer, The formation of Uranus and Neptune: Challenges and implications for intermediate-mass exoplanets. Astrophys. J. **789**, 69 (2014)

K. Heng, S. Tremaine, Long-lived planetesimal discs. Mon. Not. R. Astron. Soc. **401**, 867–889 (2010)

K. Hirayama, Groups of asteroids probably of common origin. Astron. J. **31**, 185–188 (1918)

A.W. Howard, G.W. Marcy, J.A. Johnson, D.A. Fischer, J.T. Wright, H. Isaacson, J.A. Valenti, J. Anderson, D.N.C. Lin, S. Ida, The occurrence and mass distribution of close-in super-Earths, Neptunes, and Jupiters. Science **330**, 653 (2010)

A.R. Howe, A. Burrows, W. Verne, Mass-radius relations and core-envelope decompositions of super-Earths and sub-Neptunes. Astrophys. J. **787**, 173 (2014)

N.K. Inamdar, H.E. Schlichting, The formation of super-Earths and mini-Neptunes with giant impacts. Mon. Not. R. Astron. Soc. **448**, 1751–1760 (2015)

A.P. Jackson, M.C. Wyatt, Debris from terrestrial planet formation: The Moon-forming collision. Mon. Not. R. Astron. Soc. **425**, 657–679 (2012)

A.P. Jackson, M.C. Wyatt, A. Bonsor, D. Veras, Debris from giant impacts between planetary embryos at large orbital radii. Mon. Not. R. Astron. Soc. **440**, 3757–3777 (2014)

D. Jewitt, H. Weaver, M. Mutchler, S. Larson, J. Agarwal, Hubble space telescope observations of Main-belt Comet (596) Scheila. Astrophys. J. Lett. **733**, 4 (2011)

B.C. Johnson, H.J. Melosh, Formation of melt droplets, melt fragments, and accretionary impact lapilli during a hypervelocity impact. Icarus **228**, 347–363 (2014)

B.C. Johnson, C.M. Lisse, C.H. Chen, H.J. Melosh, M.C. Wyatt, P. Thebault, W.G. Henning, E. Gaidos, L.T. Elkins-Tanton, J.C. Bridges, A. Morlok, A self-consistent model of the circumstellar debris created by a giant hypervelocity impact in the HD 172555 system. Astrophys. J. **761**, 45 (2012)

D. Jontof-Hutter, J.F. Rowe, J.J. Lissauer, D.C. Fabrycky, E.B. Ford, The mass of the Mars-sized exoplanet Kepler-138 b from transit timing. Nature **522**, 321–323 (2015)

M. Jutzi, SPH calculations of asteroid disruptions: The role of pressure dependent failure models. Planet. Space Sci. **107**, 3–9 (2015)

M. Jutzi, E. Asphaug, P. Gillet, J.-A. Barrat, W. Benz, The structure of the asteroid 4 Vesta as revealed by models of planet-scale collisions. Nature **494**, 207–210 (2013)
P. Kalas, J.R. Graham, M.P. Fitzgerald, M. Clampin, STIS coronagraphic imaging of Fomalhaut: Main belt structure and the orbit of Fomalhaut b. Astrophys. J. **775**, 56 (2013)
K. Keil, Geological history of Asteroid 4 Vesta: The "Smallest Terrestrial Planet", in *Asteroids III* (2002), pp. 573–584
G.M. Kennedy, M.C. Wyatt, The bright end of the exo-Zodi luminosity function: Disc evolution and implications for exo-Earth detectability. Mon. Not. R. Astron. Soc. **433**, 2334–2356 (2013)
G.M. Kennedy, M.C. Wyatt, Do two-temperature debris discs have multiple belts? Mon. Not. R. Astron. Soc. **444**, 3164–3182 (2014)
G.M. Kennedy, S.J. Murphy, C.M. Lisse, F. Ménard, M.L. Sitko, M.C. Wyatt, D.D.R. Bayliss, F.E. DeMeo, K.B. Crawford, D.L. Kim, R.J. Rudy, R.W. Russell, B. Sibthorpe, M.A. Skinner, G. Zhou, Evolution from protoplanetary to debris discs: The transition disc around HD 166191. Mon. Not. R. Astron. Soc. **438**, 3299–3309 (2014)
M.A. Kenworthy, E.E. Mamajek, Modeling giant extrasolar ring systems in eclipse and the case of J1407b: Sculpting by exomoons? Astrophys. J. **800**, 126 (2015)
S.J. Kenyon, B.C. Bromley, Detecting the dusty debris of terrestrial planet formation. Astrophys. J. Lett. **602**, 133–136 (2004)
S.J. Kenyon, B.C. Bromley, Prospects for detection of catastrophic collisions in debris disks. Astron. J. **130**, 269–279 (2005)
S.J. Kenyon, B.C. Bromley, Terrestrial planet formation. I. The transition from oligarchic growth to chaotic growth. Astron. J. **131**, 1837–1850 (2006)
S.J. Kenyon, B.C. Bromley, Variations on debris disks: Icy planet formation at 30–150 AU for 1–3 M_{solar} main-sequence stars. Astrophys. J. Suppl. Ser. **179**, 451–483 (2008)
S.J. Kenyon, B.C. Bromley, Coagulation calculations of icy planet formation around 0.1–0.5 $M_{\odot}$ stars: Super-Earths from large planetestimals. Astrophys. J. **780**, 4 (2014)
D.M. Kipping, D. Nesvorný, L.A. Buchhave, J. Hartman, G.Á. Bakos, A.R. Schmitt, The hunt for exomoons with Kepler (HEK). IV. A search for Moons around eight M dwarfs. Astrophys. J. **784**, 28 (2014)
T. Kleine, M. Touboul, B. Bourdon, F. Nimmo, K. Mezger, H. Palme, S.B. Jacobsen, Q.-Z. Yin, A.N. Halliday, Hf-W chronology of the accretion and early evolution of asteroids and terrestrial planets. Geochim. Cosmochim. Acta **73**, 5150–5188 (2009)
H.A. Knutson, B. Benneke, D. Deming, D. Homeier, A featureless transmission spectrum for the Neptune-mass exoplanet GJ436b. Nature **505**, 66–68 (2014)
E. Kokubo, S. Ida, Oligarchic growth of protoplanets. Icarus **131**, 171–178 (1998)
Q. Kral, P. Thébault, J.-C. Augereau, A. Boccaletti, S. Charnoz, Signatures of massive collisions in debris discs. A self-consistent numerical model. Astron. Astrophys. **573**, 39 (2015)
R.G. Kraus, S.T. Stewart, D.C. Swift, C.A. Bolme, R.F. Smith, S. Hamel, B.D. Hammel, D.K. Spaulding, D.G. Hicks, J.H. Eggert, G.W. Collins, Shock vaporization of silica and the thermodynamics of planetary impact events. J. Geophys. Res., Planets **117**, 9009 (2012)
L. Kreidberg, J.L. Bean, J.-M. Désert, B. Benneke, D. Deming, K.B. Stevenson, S. Seager, Z. Berta-Thompson, A. Seifahrt, D. Homeier, Clouds in the atmosphere of the super-Earth exoplanet GJ1214b. Nature **505**, 69–72 (2014)
A.V. Krivov, M. Sremčević, F. Spahn, Evolution of a Keplerian disk of colliding and fragmenting particles: A kinetic model with application to the Edgeworth Kuiper belt. Icarus **174**, 105–134 (2005)
T. Kubo-Oka, K. Nakazawa, Gradual increase in the obliquity of Uranus due to tidal interaction with a hypothetical retrograde satellite. Icarus **114**, 21–32 (1995)
J.D. Larwood, P.G. Kalas, Close stellar encounters with planetesimal discs: The dynamics of asymmetry in the β Pictoris system. Mon. Not. R. Astron. Soc. **323**, 402–416 (2001)
J. Lebreton, R. van Lieshout, J.-C. Augereau, O. Absil, B. Mennesson, M. Kama, C. Dominik, A. Bonsor, J. Vandeportal, H. Beust, D. Defrère, S. Ertel, V. Faramaz, P. Hinz, Q. Kral, A.-M. Lagrange, W. Liu, P. Thébault, An interferometric study of the Fomalhaut inner debris disk. III. Detailed models of the exozodiacal disk and its origin. Astron. Astrophys. **555**, 146 (2013)
Z.M. Leinhardt, S.T. Stewart, Collisions between gravity-dominated bodies. I. Outcome regimes and scaling laws. Astrophys. J. **745**, 79 (2012)
D. Li, C.M. Telesco, C.M. Wright, The mineralogy and structure of the inner debris disk of β Pictoris. Astrophys. J. **759**, 81 (2012)
C.M. Lisse, C.A. Beichman, G. Bryden, M.C. Wyatt, On the nature of the dust in the debris disk around HD 69830. Astrophys. J. **658**, 584–592 (2007)
C.M. Lisse, C.H. Chen, M.C. Wyatt, A. Morlok, Circumstellar dust created by terrestrial planet formation in HD 113766. Astrophys. J. **673**, 1106–1122 (2008)

C.M. Lisse, C.H. Chen, M.C. Wyatt, A. Morlok, I. Song, G. Bryden, P. Sheehan, Abundant circumstellar silica dust and SiO gas created by a giant hypervelocity collision in the ∼ 12 Myr HD172555 system. Astrophys. J. **701**, 2019–2032 (2009)
T. Löhne, A.V. Krivov, J. Rodmann, Long-term collisional evolution of debris disks. Astrophys. J. **673**, 1123–1137 (2008)
E.D. Lopez, J.J. Fortney, N. Miller, How thermal evolution and mass-loss sculpt populations of super-Earths and sub-Neptunes: Application to the Kepler-11 system and beyond. Astrophys. J. **761**, 59 (2012)
C. Lovis, M. Mayor, F. Pepe, Y. Alibert, W. Benz, F. Bouchy, A.C.M. Correia, J. Laskar, C. Mordasini, D. Queloz, N.C. Santos, S. Udry, J.-L. Bertaux, J.-P. Sivan, An extrasolar planetary system with three Neptune-mass planets. Nature **441**, 305–309 (2006)
K.L. Luhman, E.E. Mamajek, The disk population of the upper Scorpius association. Astrophys. J. **758**, 31 (2012)
R.E. Lupu, K. Zahnle, M.S. Marley, L. Schaefer, B. Fegley, C. Morley, K. Cahoy, R. Freedman, J.J. Fortney, The atmospheres of earthlike planets after giant impact events. Astrophys. J. **784**, 27 (2014)
L. Malo, R. Doyon, D. Lafrenière, É. Artigau, J. Gagné, F. Baron, A. Riedel, Bayesian analysis to identify new star candidates in nearby young stellar kinematic groups. Astrophys. J. **762**, 88 (2013)
E.E. Mamajek, M.R. Meyer, An improbable solution to the underluminosity of 2M1207B: A hot protoplanet collision afterglow. Astrophys. J. Lett. **668**, 175–178 (2007)
E.E. Mamajek, A.C. Quillen, M.J. Pecaut, F. Moolekamp, E.L. Scott, M.A. Kenworthy, A. Collier Cameron, N.R. Parley, Planetary construction zones in occultation: Discovery of an extrasolar ring system transiting a young Sun-like star and future prospects for detecting eclipses by circumsecondary and circumplanetary disks. Astron. J. **143**, 72 (2012)
R.A. Marcus, S.T. Stewart, D. Sasselov, L. Hernquist, Collisional stripping and disruption of super-Earths. Astrophys. J. Lett. **700**, 118–122 (2009)
G.W. Marcy, H. Isaacson, A.W. Howard, J.F. Rowe, J.M. Jenkins, S.T. Bryson, D.W. Latham, S.B. Howell, T.N. Gautier III, N.M. Batalha, L. Rogers, D. Ciardi, D.A. Fischer, R.L. Gilliland, H. Kjeldsen, J. Christensen-Dalsgaard, D. Huber, W.J. Chaplin, S. Basu, L.A. Buchhave, S.N. Quinn, W.J. Borucki, D.G. Koch, R. Hunter, D.A. Caldwell, J. Van Cleve, R. Kolbl, L.M. Weiss, E. Petigura, S. Seager, T. Morton, J.A. Johnson, S. Ballard, C. Burke, W.D. Cochran, M. Endl, P. MacQueen, M.E. Everett, J.J. Lissauer, E.B. Ford, G. Torres, F. Fressin, T.M. Brown, J.H. Steffen, D. Charbonneau, G.S. Basri, D.D. Sasselov, J. Winn, R. Sanchis-Ojeda, J. Christiansen, E. Adams, C. Henze, A. Dupree, D.C. Fabrycky, J.J. Fortney, J. Tarter, M.J. Holman, P. Tenenbaum, A. Shporer, P.W. Lucas, W.F. Welsh, J.A. Orosz, T.R. Bedding, T.L. Campante, G.R. Davies, Y. Elsworth, R. Handberg, S. Hekker, C. Karoff, S.D. Kawaler, M.N. Lund, M. Lundkvist, T.S. Metcalfe, A. Miglio, V. Silva Aguirre, D. Stello, T.R. White, A. Boss, E. Devore, A. Gould, A. Prsa, E. Agol, T. Barclay, J. Coughlin, E. Brugamyer, F. Mullally, E.V. Quintana, M. Still, S.E. Thompson, D. Morrison, J.D. Twicken, J.-M. Désert, J. Carter, J.R. Crepp, G. Hébrard, A. Santerne, C. Moutou, C. Sobeck, D. Hudgins, M.R. Haas, P. Robertson, J. Lillo-Box, D. Barrado, Masses, radii, and orbits of small Kepler planets: The transition from gaseous to rocky planets. Astrophys. J. Suppl. Ser. **210**, 20 (2014)
M.M. Marinova, O. Aharonson, E. Asphaug, Mega-impact formation of the Mars hemispheric dichotomy. Nature **453**, 1216–1219 (2008)
M.M. Marinova, O. Aharonson, E. Asphaug, Geophysical consequences of planetary-scale impacts into a Mars-like planet. Icarus **211**, 960–985 (2011)
A. Mastrobuono-Battisti, H.B. Perets, S.N. Raymond, A primordial origin for the compositional similarity between the Earth and the Moon. Nature **520**, 212–215 (2015)
B.C. Matthews, J.J. Kavelaars, Insights into planet formation from debris disks. I. The solar system as an archetype for planetesimal evolution. Space Sci. Rev. (2016, this issue)
B.C. Matthews, A.V. Krivov, M.C. Wyatt, G. Bryden, C. Eiroa, Observations, modeling, and theory of debris disks, in *Protostars and Planets VI* (2014), pp. 521–544
M. Mayor, M. Marmier, C. Lovis, S. Udry, D. Ségransan, F. Pepe, W. Benz, J.-L. Bertaux, F. Bouchy, X. Dumusque, G. Lo Curto, C. Mordasini, D. Queloz, N.C. Santos, The HARPS search for southern extra-solar planets XXXIV. Occurrence, mass distribution and orbital properties of super-Earths and Neptune-mass planets, ArXiv e-prints (2011). arXiv:1109.2497
W.B. McKinnon, On the origin of the Pluto-Charon binary. Astrophys. J. Lett. **344**, 41–44 (1989)
C. Melis, B. Zuckerman, J.H. Rhee, I. Song, The age of the HD 15407 system and the epoch of final catastrophic mass accretion onto terrestrial planets around Sun-like stars. Astrophys. J. Lett. **717**, 57–61 (2010)
C. Melis, B. Zuckerman, J.H. Rhee, I. Song, S.J. Murphy, M.S. Bessell, Rapid disappearance of a warm, dusty circumstellar disk. Nature **487**, 74–76 (2012)
H.J. Melosh, A.M. Vickery, Melt droplet formation in energetic impact events. Nature **350**, 494–497 (1991)

H.Y.A. Meng, G.H. Rieke, K.Y.L. Su, V.D. Ivanov, L. Vanzi, W. Rujopakarn, Variability of the infrared excess of extreme debris disks. Astrophys. J. Lett. **751**, 17 (2012)
H.Y.A. Meng, K.Y.L. Su, G.H. Rieke, D.J. Stevenson, P. Plavchan, W. Rujopakarn, C.M. Lisse, S. Poshyachinda, D.E. Reichart, Large impacts around a solar-analog star in the era of terrestrial planet formation. Science **345**, 1032–1035 (2014)
H.Y.A. Meng, K.Y.L. Su, G.H. Rieke, W. Rujopakarn, G. Myers, M. Cook, E. Erdelyi, C. Maloney, J. McMath, G. Persha, S. Poshyachinda, D.E. Reichart, Planetary collisions outside the solar system: Time domain characterization of extreme debris disks. Astrophys. J. **805**, 77 (2015)
M.R. Meyer, J.M. Carpenter, E.E. Mamajek, L.A. Hillenbrand, D. Hollenbach, A. Moro-Martin, J.S. Kim, M.D. Silverstone, J. Najita, D.C. Hines, I. Pascucci, J.R. Stauffer, J. Bouwman, D.E. Backman, Evolution of mid-infrared excess around Sun-like stars: Constraints on models of terrestrial planet formation. Astrophys. J. Lett. **673**, 181–184 (2008)
E. Miller-Ricci, M.R. Meyer, S. Seager, L. Elkins-Tanton, On the emergent spectra of hot protoplanet collision afterglows. Astrophys. J. **704**, 770–780 (2009)
D. Nesvorný, W.F. Bottke Jr., L. Dones, H.F. Levison, The recent breakup of an asteroid in the main-belt region. Nature **417**, 720–771 (2002)
N. Nikolov, F. Sainsbury-Martinez, Radial velocity eclipse mapping of exoplanets. ArXiv e-prints (2015)
F. Nimmo, S.D. Hart, D.G. Korycansky, C.B. Agnor, Implications of an impact origin for the martian hemispheric dichotomy. Nature **453**, 1220–1223 (2008)
D.P. O'Brien, R. Greenberg, Steady-state size distributions for collisional populations:. analytical solution with size-dependent strength. Icarus **164**, 334–345 (2003)
K. Pahlevan, D.J. Stevenson, Equilibration in the aftermath of the lunar-forming giant impact. Earth Planet. Sci. Lett. **262**, 438–449 (2007)
O. Panić, W.S. Holland, M.C. Wyatt, G.M. Kennedy, B.C. Matthews, J.F. Lestrade, B. Sibthorpe, J.S. Greaves, J.P. Marshall, N.M. Phillips, J. Tottle, First results of the SONS survey: Submillimetre detections of debris discs. Mon. Not. R. Astron. Soc. **435**, 1037–1046 (2013)
M.G. Parisi, A. Brunini, Constraints to Uranus' great collision—II. Planet. Space Sci. **45**, 181–187 (1997)
N.M. Phillips, J.S. Greaves, W.R.F. Dent, B.C. Matthews, W.S. Holland, M.C. Wyatt, B. Sibthorpe, Target selection for the SUNS and DEBRIS surveys for debris discs in the solar neighbourhood. Mon. Not. R. Astron. Soc. **403**, 1089–1101 (2010)
A. Reufer, M.M.M. Meier, W. Benz, R. Wieler, A hit-and-run giant impact scenario. Icarus **221**, 296–299 (2012)
J.H. Rhee, I. Song, B. Zuckerman, Warm dust in the terrestrial planet zone of a Sun-like Pleiades star: Collisions between planetary embryos? Astrophys. J. **675**, 777–783 (2008)
G.H. Rieke, K.Y.L. Su, J.A. Stansberry, D. Trilling, G. Bryden, J. Muzerolle, B. White, N. Gorlova, E.T. Young, C.A. Beichman, K.R. Stapelfeldt, D.C. Hines, Decay of planetary debris disks. Astrophys. J. **620**, 1010–1026 (2005)
P. Riviere-Marichalar, D. Barrado, J.-C. Augereau, W.F. Thi, A. Roberge, C. Eiroa, B. Montesinos, G. Meeus, C. Howard, G. Sandell, G. Duchêne, W.R.F. Dent, J. Lebreton, I. Mendigutía, N. Huélamo, F. Ménard, C. Pinte, HD 172555: Detection of 63 μm [OI] emission in a debris disc. Astron. Astrophys. **546**, 8 (2012)
A.C. Rizzuto, M.J. Ireland, D.B. Zucker, WISE circumstellar discs in the young Sco-Cen association. Mon. Not. R. Astron. Soc. **421**, 97–101 (2012)
L.A. Rogers, Most 1.6 Earth-radius planets are not rocky. Astrophys. J. **801**, 41 (2015)
P. Rosenblatt, The origin of the Martian moons revisited. Astron. Astrophys. Rev. **19**, 44 (2011)
P. Rosenblatt, S. Charnoz, On the formation of the martian moons from a circum-martian accretion disk. Icarus **221**, 806–815 (2012)
C.T. Russell, C.A. Raymond, A. Coradini, H.Y. McSween, M.T. Zuber, A. Nathues, M.C. De Sanctis, R. Jaumann, A.S. Konopliv, F. Preusker, S.W. Asmar, R.S. Park, R. Gaskell, H.U. Keller, S. Mottola, T. Roatsch, J.E.C. Scully, D.E. Smith, P. Tricarico, M.J. Toplis, U.R. Christensen, W.C. Feldman, D.J. Lawrence, T.J. McCoy, T.H. Prettyman, R.C. Reedy, M.E. Sykes, T.N. Titus, Dawn at Vesta: Testing the protoplanetary paradigm. Science **336**, 684 (2012)
V.S. Safronov, *Evolution of the Protoplanetary Cloud and Formation of the Earth and Planets*. 1972
J. Salmon, R.M. Canup, Lunar accretion from a Roche-interior fluid disk. Astrophys. J. **760**, 83 (2012)
H.E. Schlichting, R. Sari, The creation of Haumea's collisional family. Astrophys. J. **700**, 1242–1246 (2009)
H.E. Schlichting, R. Sari, A. Yalinewich, Atmospheric mass loss during planet formation: The importance of planetesimal impacts. Icarus **247**, 81–94 (2015)
A. Schneider, I. Song, C. Melis, B. Zuckerman, M. Bessell, T. Hufford, S. Hinkley, The nearby, young, isolated, dusty star HD 166191. Astrophys. J. **777**, 78 (2013)
S. Seager, M. Kuchner, C.A. Hier-Majumder, B. Militzer, Mass-radius relationships for solid exoplanets. Astrophys. J. **669**, 1279–1297 (2007)

Y. Sekine, H. Genda, Giant impacts in the Saturnian system: A possible origin of diversity in the inner mid-sized satellites. Planet. Space Sci. **63**, 133–138 (2012)
M.R. Showalter, D.P. Hamilton, Resonant interactions and chaotic rotation of Pluto's small moons. Nature **522**, 45–49 (2015)
N. Siegler, J. Muzerolle, E.T. Young, G.H. Rieke, E.E. Mamajek, D.E. Trilling, N. Gorlova, K.Y.L. Su, Spitzer 24 μm observations of open cluster IC 2391 and debris disk evolution of FGK stars. Astrophys. J. **654**, 580–594 (2007)
D.E. Smith, M.T. Zuber, S.C. Solomon, R.J. Phillips, J.W. Head, J.B. Garvin, W.B. Banerdt, D.O. Muhleman, G.H. Pettengill, G.A. Neumann, F.G. Lemoine, J.B. Abshire, O. Aharonson, C.D. Brown, S.A. Hauck, A.B. Ivanov, P.J. McGovern, H.J. Zwally, T.C. Duxbury, The global topography of Mars and implications for surface evolution. Science **284**, 1495 (1999)
R. Smith, L.J. Churcher, M.C. Wyatt, M.M. Moerchen, C.M. Telesco, Resolved debris disc emission around η Telescopii: A young solar system or ongoing planet formation? Astron. Astrophys. **493**, 299–308 (2009a)
R. Smith, M.C. Wyatt, C.A. Haniff, Resolving the hot dust around HD69830 and η Corvi with MIDI and VISIR. Astron. Astrophys. **503**, 265–279 (2009b)
R. Smith, M.C. Wyatt, C.A. Haniff, Resolving the terrestrial planet forming regions of HD 113766 and HD 172555 with MIDI. Mon. Not. R. Astron. Soc. **422**, 2560–2580 (2012)
I.A.G. Snellen, B.R. Brandl, R.J. de Kok, M. Brogi, J. Birkby, H. Schwarz, Fast spin of the young extrasolar planet β Pictoris b. Nature **509**, 63–65 (2014)
I. Song, B. Zuckerman, A.J. Weinberger, E.E. Becklin, Extreme collisions between planetesimals as the origin of warm dust around a Sun-like star. Nature **436**, 363–365 (2005)
C.C. Stark, G. Schneider, A.J. Weinberger, J.H. Debes, C.A. Grady, H. Jang-Condell, M.J. Kuchner, Revealing asymmetries in the HD 181327 debris disk: A recent massive collision or interstellar medium warping. Astrophys. J. **789**, 58 (2014)
S.T. Stewart, Z.M. Leinhardt, Collisions between gravity-dominated bodies. II. The diversity of impact outcomes during the end stage of planet formation. Astrophys. J. **751**, 32 (2012)
K.Y.L. Su, G.H. Rieke, J.A. Stansberry, G. Bryden, K.R. Stapelfeldt, D.E. Trilling, J. Muzerolle, C.A. Beichman, A. Moro-Martin, D.C. Hines, M.W. Werner, Debris disk evolution around a stars. Astrophys. J. **653**, 675–689 (2006)
K.Y.L. Su, G.H. Rieke, R. Malhotra, K.R. Stapelfeldt, A.M. Hughes, A. Bonsor, D.J. Wilner, Z. Balog, D.M. Watson, M.W. Werner, K.A. Misselt, Asteroid belts in debris disk twins: Vega and Fomalhaut. Astrophys. J. **763**, 118 (2013)
C.M. Telesco, R.S. Fisher, M.C. Wyatt, S.F. Dermott, T.J.J. Kehoe, S. Novotny, N. Mariñas, J.T. Radomski, C. Packham, J. De Buizer, T.L. Hayward, Mid-infrared images of β Pictoris and the possible role of planetesimal collisions in the central disk. Nature **433**, 133–136 (2005)
P. Thébault, J.C. Augereau, H. Beust, Dust production from collisions in extrasolar planetary systems. The inner beta Pictoris disc. Astron. Astrophys. **408**, 775–788 (2003)
R. Visser, E.F. van Dishoeck, J.H. Black, The photodissociation and chemistry of CO isotopologues: Applications to interstellar clouds and circumstellar disks. Astron. Astrophys. **503**, 323–343 (2009)
K.J. Walsh, A. Morbidelli, S.N. Raymond, D.P. O'Brien, A.M. Mandell, A low mass for Mars from Jupiter's early gas-driven migration. Nature **475**, 206–209 (2011)
L.M. Weiss, G.W. Marcy, The mass-radius relation for 65 exoplanets smaller than 4 Earth radii. Astrophys. J. Lett. **783**, 6 (2014)
G.W. Wetherill, Collisions in the asteroid belt. J. Geophys. Res. **72**, 2429 (1967)
D.E. Wilhelms, S.W. Squyres, The martian hemispheric dichotomy may be due to a giant impact. Nature **309**, 138–140 (1984)
A. Wolfgang, E. Lopez, How rocky are they? The composition distribution of Kepler's sub-Neptune planet candidates within 0.15 AU. Astrophys. J. **806**, 183 (2015)
M.C. Wyatt, Resonant trapping of planetesimals by planet migration: Debris disk clumps and Vega's similarity to the solar system. Astrophys. J. **598**, 1321–1340 (2003)
M.C. Wyatt, Dust in resonant extrasolar Kuiper belts: Grain size and wavelength dependence of disk structure. Astrophys. J. **639**, 1153–1165 (2006)
M.C. Wyatt, Evolution of debris disks. Annu. Rev. Astron. Astrophys. **46**, 339–383 (2008)
M.C. Wyatt, W.R.F. Dent, Collisional processes in extrasolar planetesimal discs - dust clumps in Fomalhaut's debris disc. Mon. Not. R. Astron. Soc. **334**, 589–607 (2002)
M.C. Wyatt, R. Smith, J.S. Greaves, C.A. Beichman, G. Bryden, C.M. Lisse, Transience of hot dust around Sun-like stars. Astrophys. J. **658**, 569–583 (2007a)
M.C. Wyatt, R. Smith, K.Y.L. Su, G.H. Rieke, J.S. Greaves, C.A. Beichman, G. Bryden, Steady state evolution of debris disks around a stars. Astrophys. J. **663**, 365–382 (2007b)

M.C. Wyatt, M. Booth, M.J. Payne, L.J. Churcher, Collisional evolution of eccentric planetesimal swarms. Mon. Not. R. Astron. Soc. **402**, 657–672 (2010)
M.C. Wyatt, C.J. Clarke, M. Booth, Debris disk size distributions: Steady state collisional evolution with Poynting-Robertson drag and other loss processes. Celest. Mech. Dyn. Astron. **111**, 1–28 (2011)
M.C. Wyatt, O. Panić, G.M. Kennedy, L. Matrà, Five steps in the evolution from protoplanetary to debris disk. Astrophys. Space Sci. **357**, 103 (2015)
K. Zahnle, N. Arndt, C. Cockell, A. Halliday, E. Nisbet, F. Selsis, N.H. Sleep, Emergence of a Habitable planet. Space Sci. Rev. **129**, 35–78 (2007)
B. Zuckerman, C. Melis, J.H. Rhee, A. Schneider, I. Song, Stellar membership and dusty debris disks in the α persei cluster. Astrophys. J. **752**, 58 (2012)
J.I. Zuluaga, D.M. Kipping, M. Sucerquia, J.A. Alvarado, A novel method for identifying exoplanetary rings. Astrophys. J. Lett. **803**, 14 (2015)